STANFORD RESEARCH INSTITUTE
MENLO PARK, CALIFORNIA

March 1964

BIOLOGICAL AND RADIOLOGICAL EFFECTS OF FALLOUT FROM NUCLEAR EXPLOSIONS

Chapter 1: The Nature of Fallout
Chapter 2: Formation of Fallout Particles

By: CARL F. MILLER

SRI Project No. IMU-4536

CONTRACT NO. OCD-OS-63-149
OCD SUBTASK NO. 3110A

Prepared for:

OFFICE OF CIVIL DEFENSE
DEPARTMENT OF DEFENSE
WASHINGTON, D.C. 20301

This report has been reviewed by the Office of Civil Defense and approved for publication.

2.2 The Structure and Composition of Individual Fallout Particles

Information on the structure and composition of individual fallout particles is obtained mainly from two types of observations: (1) petrographic and radiographic analyses of thin sections of fallout particles and (2) radiochemical and chemical analyses of fallout particles. The results of analyses of single fallout particles contribute more to the understanding of the fallout formation process than any other types of analysis. The major limitation in the analyses of single particles is that the methods are not applicable to the study of particles of less than about 100 microns in diameter (and usually larger) for the petrographic methods and of particles with less than a given radioactive content for the radiochemical methods. The pertinent results from the petrographic and radiographic studies are summarized here, and a description of the experimental techniques follows the summary.

2.2.1 Low Yield, Surface Shot, Silicate Soil

Particles from Operation Jangle in 1951 were analyzed by Adams, Poppoff, and Wallace[2] of the U.S. Naval Radiological Defense Laboratory (NRDL) and by others.[3,4,5] The results of these analyses are the only ones available on fallout from a detonation on the surface of a silicate soil. The particles studied ranged in size from 500 to 10,000 microns in diameter and were selected on the basis of activity content. Thus the results apply to the larger and most highly radioactive of the fallout particles. The observations were made on thin sections about 30 microns thick taken from the central region of the particles (see Figures 2.1 and 2.2).

The findings are summarized as follows:

1. In thin section, almost all of the fallout particles consisted throughout of a transparent glass (i.e. a fused silicate mass). Many contained fragments of unmelted mineral grains and air bubbles inside the glass. The mineral grains composed perhaps a few percent of the volume of a particle, and the bubbles or voids composed something like two to four times the volume of the mineral grains. Some particles, in the glass phase, contained neither mineral grains nor air bubbles, and no radioactivity was found in the unmelted mineral grains.

2. Most of the mineral grains in the glass particles were too small to be easily identified with the petrographic microscope.

Figure 2.1
THIN SECTIONS AND RADIOGRAPHS OF SOME FALLOUT PARTICLES FROM A SMALL-YIELD SURFACE SHOT AT THE NEVADA TEST SITE. THE PARTICLES ARE A TRANSPARENT, GREEN-YELLOW GLASS WITH THE RADIOACTIVITY DISTRIBUTED MORE OR LESS UNIFORMLY THROUGHOUT THEIR VOLUMES

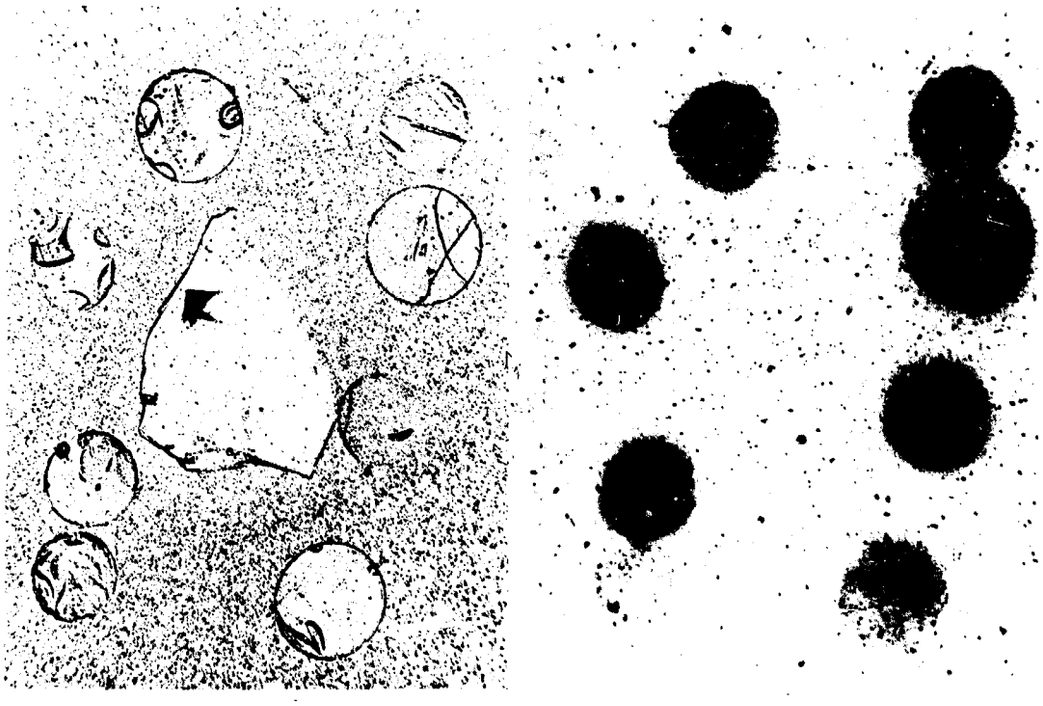

Figure 2.2
THIN SECTION AND RADIOGRAPH OF A FALLOUT PARTICLE FROM A SMALL-YIELD SURFACE SHOT AT THE NEVADA TEST SITE. THE PARTICLE IS A TRANSPARENT YELLOW-BROWN GLASS WITH MANY INCLUSIONS OF GAS BUBBLES AND UNMELTED MINERAL GRAINS. THE RADIOACTIVITY IS DISTRIBUTED IRREGULARLY THROUGHOUT THE GLASS PHASE OF THE PARTICLE

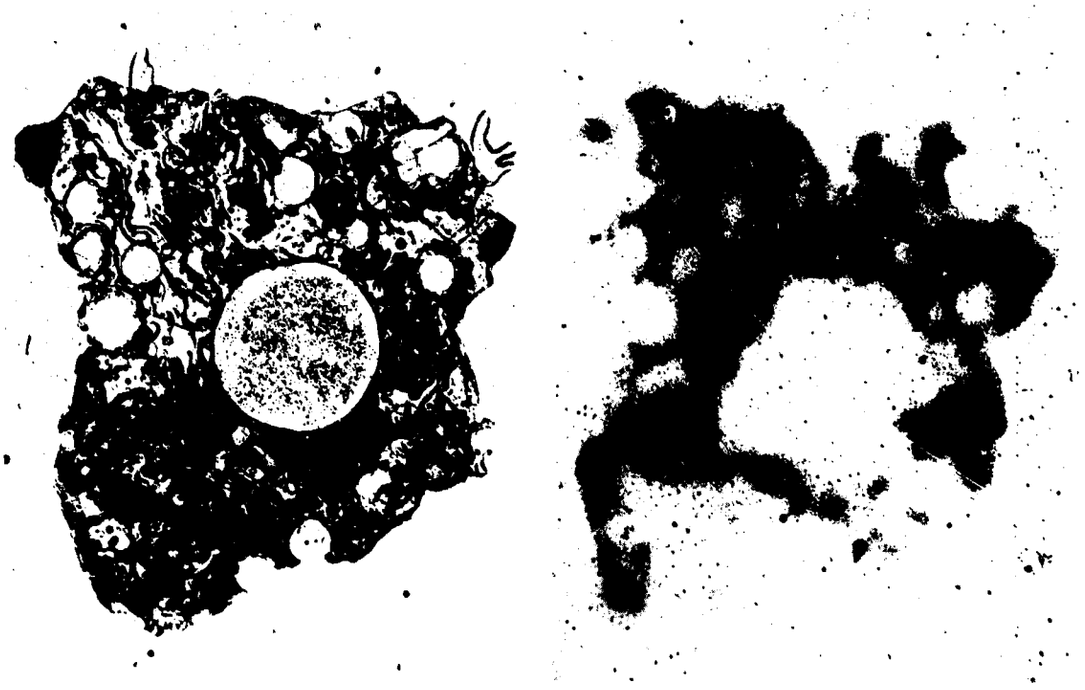

Those that were large enough were identified as quartz or feldspar; about 75 percent of the soil at the shot point consisted of these two minerals. Most of the grains were smaller than that of the native soil, appeared to be shattered, generally gave no appearance of being melted, and generally were found scattered at random throughout the glass phase.

3. A fairly large fraction of the particles were spherical or spheroidal; some were true spheres of about 500 microns diameter. The smaller of the particle sizes studied contained fewer mineral grains and voids than the larger irregularly-shaped particles.

4. The exterior appearance of the spherical particles varied from a transparent yellow-green color to a light brown color, and the radioactivity was distributed more or less homogeneously throughout their volume. Many of the spheres had smaller spheres attached or partially fused to their surfaces.

5. The exterior appearance of the irregular particles was the same as that of the native soil mineral grains but, in the glass phase, the radioactivity was distributed in an irregular manner throughout the irregular particle.

The study indicated that the large glass particles containing significant amounts of radioactivity could not have been formed by direct vapor condensation of the silicate glass. Electron micrographs of fallout collected on air filters revealed the presence of spheres having diameters of the order of 0.1 micron. Theoretical calculations such as those of Stewart[6] on the condensation of such materials as iron and fission products (in air) in the cooling fireball give particle diameters of the order of 0.1 micron. In his calculation, Stewart assumed a fireball containing 25 tons of iron in a radius of 500 feet and that the growth of the particles was a combination of condensation and coagulation. Stewart obtained a modal diameter of 0.2 micron for the iron oxide particles.

Simple kinetic theory equations that describe the growth of particles by collision processes give particle-diameter values, for the formation of particles of a given size in the vapor condensation process, that range from about 0.001 to 0.1 micron, depending on various assumed values of the initial vapor density. Thus the small spherical particles in the NRDL study, with diameters of the order of 0.1 micron, probably resulted from direct vapor condensation plus some growth by particle impaction in the liquid state.

The large spherical particles (containing radioactivity but very few or no mineral grains and no voids) were most likely either mineral grains heated to temperatures near the boiling point of the glass so that the glass became fluid or were from a layer of liquid soil, at a point nearest the initial fireball gases, that formed particles when the crater material was violently pulled upward as the fireball rose in the air. The more irregular particles containing the shattered but unmelted mineral grains could have been formed by the violent mixing of the molten glass with the grains of soil minerals that were originally outside the melted zone. The voids also could have been produced in this violent mixing process as well as by the partial vaporization of volatile constituents in the melted soil that was not sufficiently hot and fluid to permit the escape of these gases.

2.2.2 Low Yield, Underground Shot, Silicate Soil

Particles from a low-yield underground shot were also examined by Adams, Poppoff, and Wallace. None of the larger particles were spherical. However, fused glass spheres in the small size range (less than 100 microns in diameter) were observed. Superficially, most of the radioactive particles looked like the original soil minerals of the detonation area. They were usually a light brown in color and opaque. In thin section, they were transparent and colorless, had the glass structure found for the surface-shot fallout, but contained a much higher concentration of unmelted mineral grains and voids.

2.2.3 Large Yield, Surface Shot, Coral

Particles available for analysis from detonations of large-yield weapons on the surface of land areas are restricted to those of the fallout produced from coral atolls. The coral reefs are, of course, composed largely of calcium carbonate in the form of aragonite.[7] The findings of C. E. Adams,[8] from analyses of particles obtained from the Mike Shot of Operation Ivy, the first large thermonuclear detonation, are summarized as follows:

a. The particles available for study were grains of a solid white material whose diameters range from [illegible]00 microns to less than 25 microns. (Those selected [illegible] petrographic and radiographic analyses had diameters between about 750 and 1,500 microns.)

2. The principal constituents, as determined from x-ray diffraction patterns of powders prepared from a group of particles, were calcium carbonate, in both the calcite and aragonite forms, and calcium hydroxide. Sodium chloride and magnesium oxide were also present but the calcium carbonate and hydroxide compounds were in highest abundance. Small amounts of calcium nitrate were also found on the exterior of some particles.

3. Most of the particles were composed of calcium hydroxide, with a surface layer of calcium carbonate of the calcite structure. The thickness of the surface calcium carbonate layer, on particles exposed to the open air, increased with time. These particles were generally angular in shape.

4. A few particles consisted of only calcium carbonate (aragonite structure).

5. The radiographs of the thin sections of the particles showed that the radioactivity was usually concentrated in a band near the outer surface of the particle (see Figure 2.3). However, a significant fraction of the particles studied had radioactivity distributed more or less uniformly throughout their volumes. These distributions were not found to be related to the chemical or physical structure of the particles.

This information on fallout from detonations on coral was later added to; analyses were made of particles collected from other thermonuclear detonations and by improved sampling methods and coverage. A general discussion of all the results was given by Admas, Farlow, and Schell.[9] The findings pertinent to fallout from large detonations on coral are:

1. The angular particles found predominating in the Operation Ivy Mike Shot fallout were always observed. Variations in this general type of angular particles included some particles containing a core of unaltered calcium carbonate and others with many small reddish-orange-to-black spheres adhering to the particle surface.

2. Occasionally, unaltered coral particles were found that had small black spheres attached to their surfaces (see Figure 2.4). The size of the small spheres generally ranged from submicroscopic up to about 10 microns in diameter.

Figure 2.3
THIN SECTION AND RADIOGRAPH OF AN ANGULAR FALLOUT PARTICLE FROM A LARGE-YIELD SURFACE SHOT AT THE ENIWETOK PROVING GROUNDS. THIS PARTICLE IS COMPOSED ALMOST ENTIRELY OF CALCIUM HYDROXIDE WITH A THIN OUTER LAYER OF CALCIUM CARBONATE. THE RADIOACTIVITY HAS COLLECTED ON THE SURFACE AND HAS DIFFUSED A SHORT DISTANCE INTO THE PARTICLE

Figure 2.4
SECTION OF A FALLOUT PARTICLE FROM A LARGE-YIELD SURFACE SHOT AT THE ENIWETOK PROVING GROUND. THE SMALL, BLACK, RADIOACTIVE SPHERES SHOWN ADHERING TO THE SURFACE OF A CORAL SAND GRAIN ARE FORMED BY VAPOR CONDENSATION, WITH SUBSEQUENT GROWTH BY COAGULATION, OF MATERIALS VAPORIZED IN THE FIREBALL

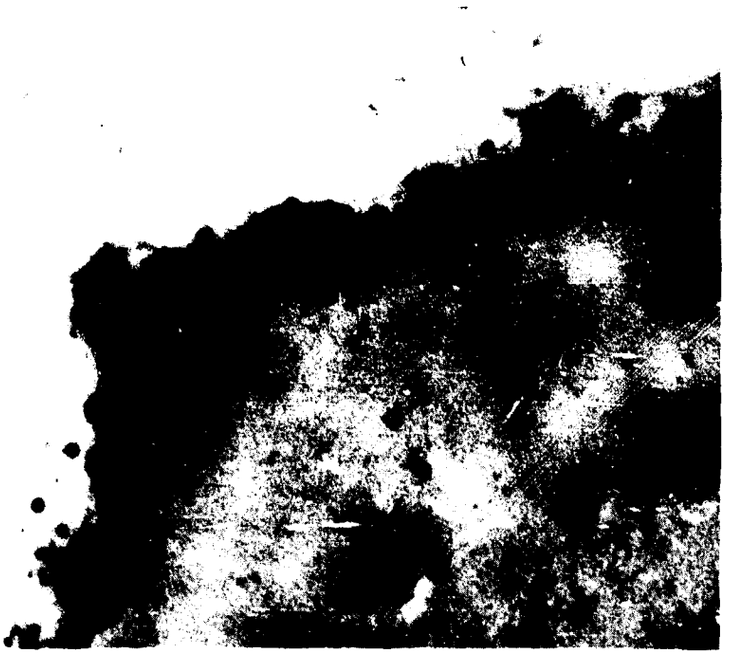

3. The third general type of particle found was spherical; it was composed of calcium oxide that, by the time of analysis, had partially hydrated to calcium hydroxide. The surface was covered with a thin layer of calcium carbonate in the calcite form. In these spherical forms, the radioactivity was usually distributed more or less uniformly throughout the particle (see Figure 2.5).

4. The fourth general type of particle found was a very fragile fluffy particle similar to a snowflake. (Most of these apparently broke easily, either on landing in the collectors or in the handling and shipping of the samples.)

The angular particles, the ones having the irregular shape of fractured coral grains, must have been heated to temperatures higher than 800 to 900°C, since this range of temperatures decarbonates the calcium carbonate. However, the angular particles did not reach the temperature of 2590°C required to melt the calcium oxide. The microporous calcium oxide was hydrated by atmospheric water after it cooled and during its fall to the earth. The calcium carbonate layer in the calcite form must have been formed from the carbon dioxide of the atmosphere after the particle had cooled, since calcite is the stable structure formed by this reaction at temperatures less than 30°C.

The small orange-red-to-black spheres were vapor-condensed particles consisting of a mixture of calcium, iron, and fission-produced oxides. Since it was later found that a large fraction of the activity was in ionic form and could be leached from the angular particles lacking the spheres on their surfaces, it is likely that these radioactive fission products were present in molecular or ionic form in the structure of the particle. The band of activity around the edge of the particle indicates that some inward diffusion must have occurred.

The small particles on the surfaces of the larger ones, however, did not lose activity by diffusion. Hence, some of the activity in these irregular particles must have been collected by the vapor condensation of fission-product elements in their molecular form and some from collisions with vapor-condensed solid (or liquid) particles ranging from molecular size to 10 microns in diameter. The solid calcium oxide, in the presence of carbon dioxide, can exist between 900°C and 2590°C, and many of the fission-product oxides can condense from a vapor phase in this temperature range. The iron, for production of the vapor-condensed spheres, came from the structures around the test device, and the calcium oxide from the vaporized coral at shot point.

Figure 2.5
THIN SECTION AND RADIOGRAPH OF A SPHERICAL FALLOUT PARTICLE FROM A LARGE-YIELD SURFACE SHOT AT THE ENIWETOK PROVING GROUND. THIS PARTICLE IS COMPOSED ALMOST ENTIRELY OF CALCIUM OXIDE WITH A THIN SURFACE LAYER OF CALCIUM HYDROXIDE AND CALCIUM CARBONATE. THE RADIOACTIVITY IS DISTRIBUTED MORE OR LESS UNIFORMLY THROUGHOUT THE VOLUME OF THE PARTICLE

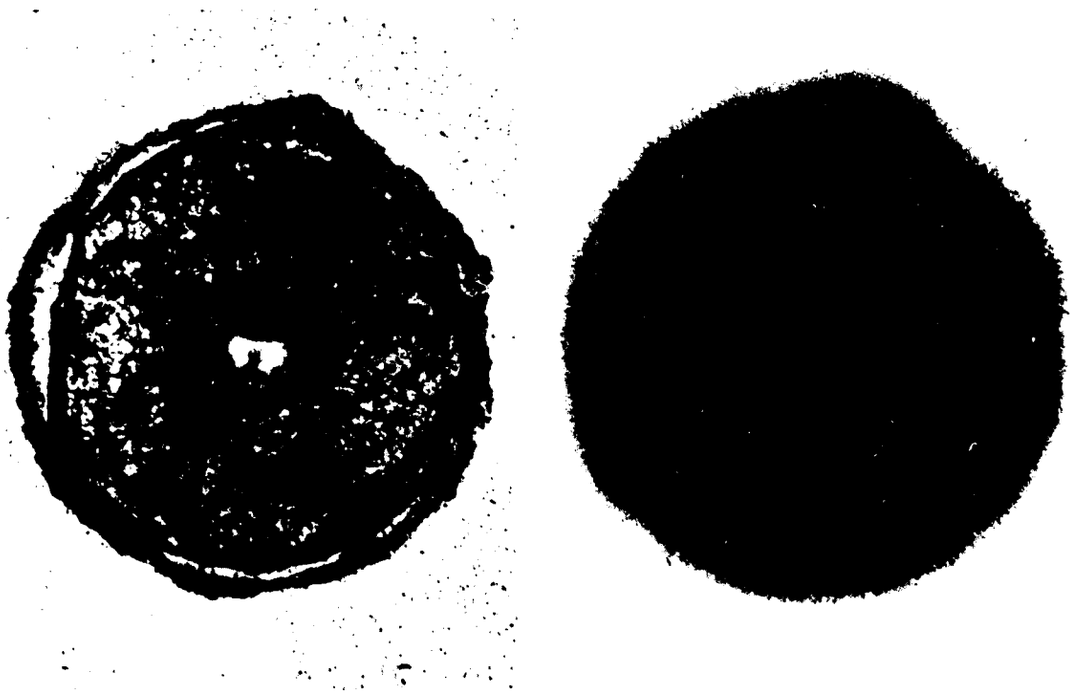

The spherical particles were formed from coral particles heated to temperatures between 2590°C, the melting point of calcium oxide, and about 3500°C, its boiling point (in the presence of about one atmosphere of oxygen). Since this temperature range is not large and would be of short duration, spherical particles were neither formed nor found in great abundance or in large size ranges in coral fallout. Also, melting would destroy the porous structure of the calcium oxide so that the hydration process would be much slower; hence, in these spherical coral particles, a large fraction of the oxide would not be converted to hydroxide until after a long exposure to humid atmospheric conditions.

Hydration of the fused calcium oxide involves an increase by a factor of 2 in the volume of the solid, resulting in a rupture of the crystal to the crumbly, fluffy structure. Hence the fragile fluffy particles may have formed from small vapor-condensed calcium oxide particles that hydrated as they fell and agglomerated with other similar particles. Some of these particles may have been formed from larger melted particles that collided with water drops in their fall and thus completely hydrated to the observed structure.

2.2.4 Tower Shot, Silicate Soil

Fallout particles from tower shots over both coral and silicate soils have been collected and analyzed. The results of analyses on particles from a tower detonation over silicate soils by C. E. Adams and J. P. Wittman[10] are summarized as follows:

1. The particle size used in the study ranged from 140 to 1,750 microns in diameter. Most of the particles were brown-to-black spheres or spheroids but some were irregular in shape (see Figure 2.6). Most of them were magnetic. The surface luster was between dull metallic and a brilliant gloss. Their measured densities were between 1.4 and 2.9 gm/cm^3. Many of the particles had smaller spheres fused onto their surfaces.

2. In thin section, the central core of the particles was transparent glass with a color ranging from light brown to colorless (see Figure 2.7). The core was surrounded by an irregular thickness of dark brown (or black) opaque glass.

3. The glass occasionally had flow lines and, in many cases, a fairly large number of voids; the latter were responsible for the extreme variation in the observed densities. A few mineral grains were observed in the glass matrix.

Figure 2.6
TWO FALLOUT PARTICLES FROM A TOWER SHOT AT THE NEVADA TEST SITE. THE PARTICLE ON THE LEFT IS A PERFECT SPHERE WITH A HIGHLY GLOSSY SURFACE; THE ONE ON THE RIGHT HAS MANY PARTIALLY-ASSIMILATED SMALLER SPHERES ATTACHED TO ITS SURFACE. BOTH PARTICLES ARE BLACK AND MAGNETIC AND HAVE A SUPERFICIAL METALLIC APPEARANCE. THE INTERIOR STRUCTURE OF THIS TYPE OF PARTICLE IS SHOWN IN FIGURE 2.7

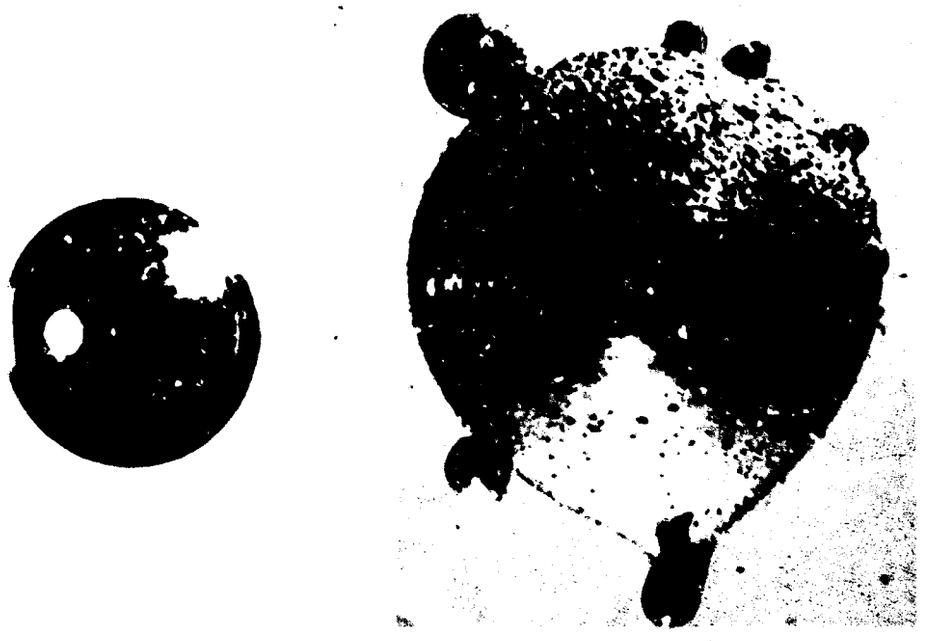

Figure 2.7
THIN SECTION AND RADIOGRAPH OF A FALLOUT PARTICLE FROM A MODERATE-YIELD TOWER SHOT AT THE NEVADA TEST SITE. THIS PARTICLE IS COMPOSED OF A TRANSPARENT GLASS CORE WITH A DARKLY COLORED IRON OXIDE GLASS OUTER ZONE. MOST OF THE RADIOACTIVITY IS CONCENTRATED IN THE OUTER ZONE

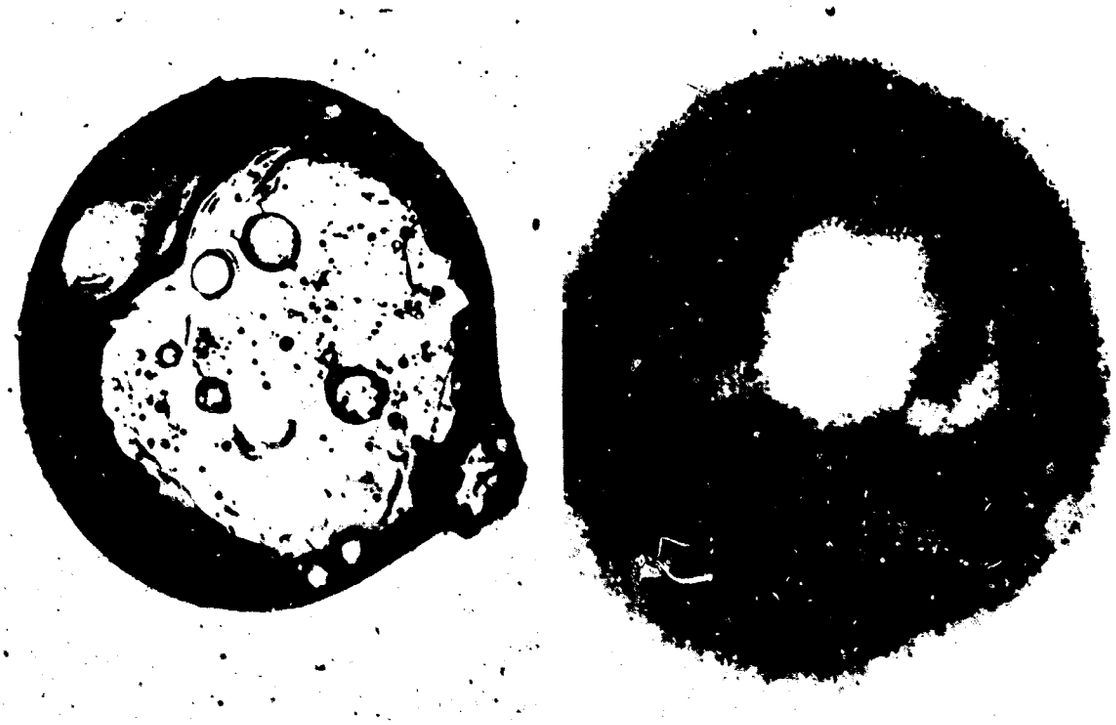

4. The radiographs showed that the radioactivity was usually more highly concentrated in the opaque glass around the core. In some particles, the core was inactive; in others, the radioactivity was distributed in a more or less random manner throughout the particle.

The strong magnetic property of these particles was due to the iron oxide (opaque) glass around the central core. The smaller particles tended to be more opaque throughout their volumes, i.e. without the transparent central core. The amount of iron oxide glass varied somewhat with weapon yield and with the tower's size or mass; the heavier tower types resulted in particles containing as much as an average of 5 percent iron by weight.

2.2.5 Tower Shot, Coral Soil

The results of analyses of particles from a tower detonation over coral soils by C. E. Adams and J. D. O'Connor[11] are summarized as follows:

1. Three general types of radioactive particles were found.

2. The most abundant type was dull black, spheroidal, weakly magnetic, and cracked and veined with white crystalline material. The sizes analyzed had diameters from about 500 to 1,000 microns. The thin sections (see Figure 2.8) showed that these particles had a central core--originally calcium oxide but partially converted to calcium hydroxide and calcium carbonate by the time of sectioning--that was surrounded by a thick layer of black opaque material identified as dicalcium ferrite ($2CaO \cdot Fe_2O_3$). The white material in the veins was found to be a mixture of calcite and vaterite, the two low-temperature crystal forms of calcium carbonate. The radioactivity was always concentrated in the dicalcium ferrite phase.

3. The second most abundant type was a magnetic black spherical particle with a glossy luster. The particles in the samples analyzed were between 250 and 500 microns in diameter and were composed mostly of magnetite (Fe_3O_4) along with some hematite (Fe_2O_3). The radioactivity was found to be more or less uniformly distributed throughout the particle volume (see Figure 2.9).

Figure 2.8
THIN SECTION AND RADIOGRAPH OF A FALLOUT PARTICLE FROM A MODERATE-YIELD TOWER SHOT AT THE ENIWETOK PROVING GROUND. THE GRAY CENTRAL AREA AND VEINS ARE REMNANTS OF THE ORIGINAL INACTIVE MELTED CALCIUM OXIDE PARTICLE. THE DARK AREAS ARE THE DICALCIUM FERRITE IN WHICH THE RADIOACTIVITY IS CONCENTRATED

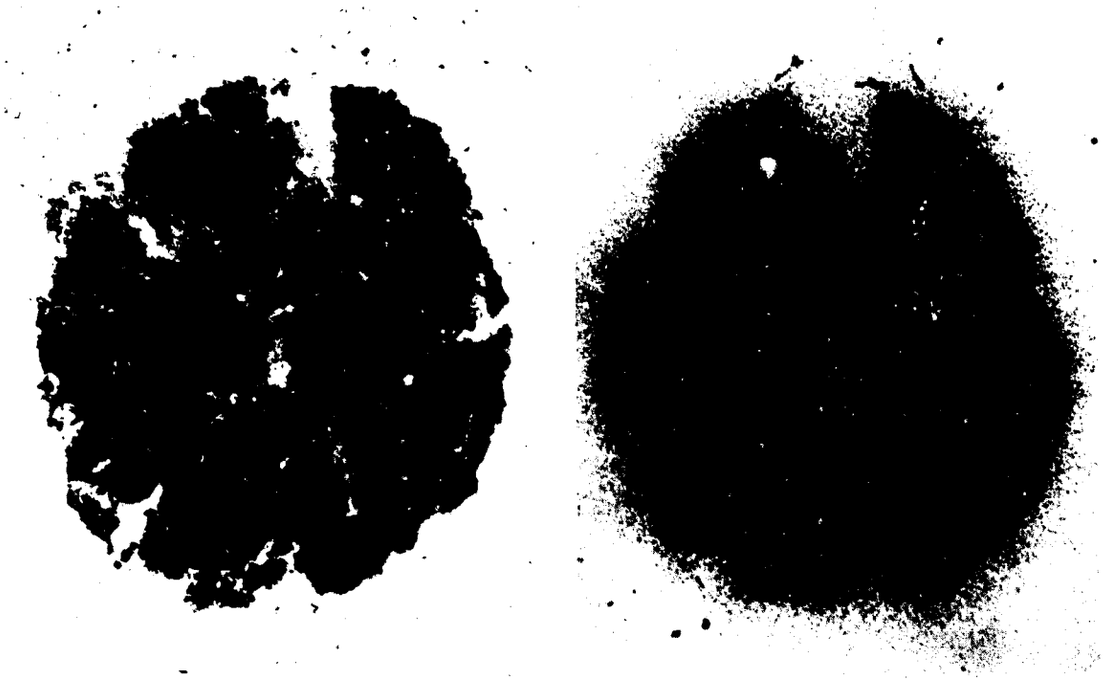

Figure 2.9
THIN SECTION AND RADIOGRAPH OF A FALLOUT PARTICLE FROM A MODERATE-YIELD TOWER SHOT AT THE ENIWETOK PROVING GROUND. THIS PARTICLE IS COMPOSED ENTIRELY OF MAGNETITE AND THE RADIOACTIVITY IS DISTRIBUTED UNIFORMLY THROUGHOUT ITS VOLUME

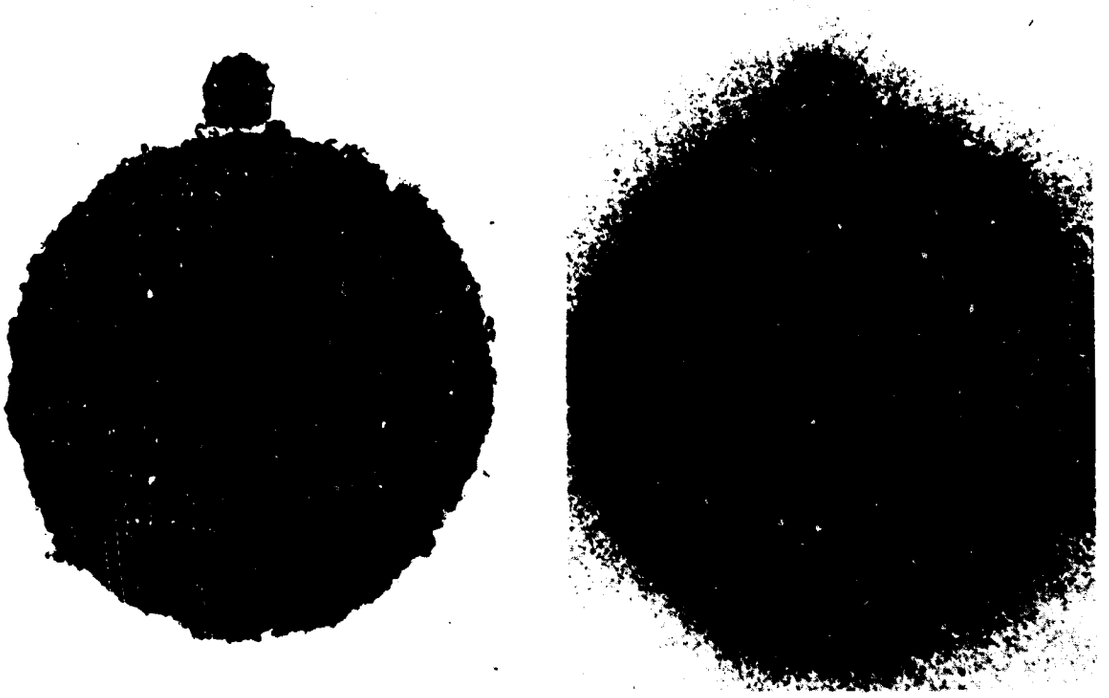

4. The third type, not very abundant, was white and irregular in shape and looked much like grains of the original coral. The thin sections showed these particles to be composed either of unaltered coral or of calcium hydroxide with a thin coating of calcium carbonate. Many small black spheres with diameters about 10 microns or less were found attached to the surface of these least abundant particles. The radioactivity, as shown by radiographs, was concentrated in these attached small black spheres.

The most abundant type of particles contained dicalcium ferrite; these could only have been formed either by the reaction between liquid calcium oxide particles and iron vapor in the presence of oxygen or by the impaction and solution of small drops of liquid iron oxide to form the dicalcium ferrite. Since the calcium oxide has a twofold volume increase on hydration to the hydroxide, the veins must have formed after the particles solidified under internal pressure resulting from the hydration of the inner core of calcium oxide. In this process, some of the hydroxide apparently diffused into the fissures where it was carbonated by atmospheric carbon dioxide.

The second most abundant type, the iron oxide particles, were probably formed during the cooling of the fireball by the oxidation of liquid iron drops (from the steel tower). Both the vaporized iron and some of the fission-product elements apparently condensed more or less simultaneously to form these particles; apparently they solidified without colliding with molten calcium oxide particles.

Since the melting temperature of magnetite is 1600°C and that of the calcium oxide is 2590°C, the two would not be present in liquid form in the temperature range 1600°C to 2590°C. In fact, the more stable liquid iron oxide (in the presence of about one atmosphere of oxygen at temperatures above the melting point) is FeO; under these conditions, its boiling point is about 3300°C. Thus the temperature range over which both liquid calcium oxide and iron oxide may exist is between about 2600°C and 3300°C. The iron came from the tower, it was located nearer to the center of the detonation than the calcium oxide that was originally coral at the base of the tower; the presence of the pure iron oxide particles indicates that the two materials did not mix homogeneously in the fireball by the time it cooled to 2600°C. The absence of calcium in the particles also indicates that the amount of calcium oxide vaporized was very small.

The third type of particle was apparently formed by collisions between the small vapor-condensed iron oxide particles and grains of coral not heated to 2590°C. Thus these least-abundant particles must have formed at later times than the other two types. The fact that the small attached particles were as large as 10 microns indicates that the initial vapor condensation process continued long enough to permit considerable coagulation.

That the pure iron oxide particles were not observed in the fallout from tower shots over silicate soil does not prove their nonexistence but that, if produced, their abundance in the fallout was very low. This is best explained by the fact that the glass from silicate minerals can exist in a liquid (i.e. fluid) state at temperatures even lower than those at which the pure iron oxide solidifies. This would permit more time for mixing in the fireball and for coagulation of the liquid drops of iron oxide and the silicate minerals. Since many of the silicate glass particles had small spheres attached or fused onto their surfaces, the process of coagulation must have continued until the surface of the particles was very viscous.

Weapon yield, the height and mass of the tower, and the boiling temperatures of the various substances are all factors in determining whether ground-surface materials are vaporized and, if they are vaporized, in determining the quantities that enter the fireball in vapor form. Most of the fallout particles from tower shots are undoubtedly derived from grains of original soil. However, in one or two cases, where the surface soil contained an appreciable amount of substances that melt at low temperatures, such as sodium carbonate, that could act as a fluxing agent, evidence of liquid puddling on the surface of the soil under the tower was observed.

2.2.6 Surface Shot, Ocean (Sea Water)

Only a few fallout particles or liquid drops from detonations on or near the surface of the ocean have been analyzed, mainly due to the fact that special analystical techniques not available early in the weapons test series had to be developed. However, special reagent films developed by Farlow[12] for analyzing liquid drops were used on a few collected samples (see Figure 2.10). The particles, collected at a single location from a detonation on a barge anchored in the lagoon at Bikini Atoll, consisted of a saturated solution of sea water salts, some suspended crystals of sodium chloride, and some insoluble solids.

Figure 2.10
PHOTOMICROGRAPH OF A DICHROMATE REAGENT FILM OF AN INDIVIDUAL LIQUID FALLOUT PARTICLE FROM A LARGE-YIELD BARGE SHOT AT THE ENIWETOK PROVING GROUND. THE SOLUBLE CHLORIDE IN THE DROP HAS REACTED WITH THE REAGENT FILM, FORMING A WHITE CIRCULAR AREA INDICATING THE AMOUNT OF CHLORIDE IN THE DROP. THE AREA OF THE CENTRAL ELLIPTICAL TRACE COVERED BY SMALL SOLID PARTICLES IS A MEASURE OF THE WATER CONTENT OF THE DROP. THE SOLIDS IN THE CENTER ARE SMALL SPHERES FORMED BY THE CONDENSATION OF THE VAPORIZED BARGE AND BALLAST MATERIALS

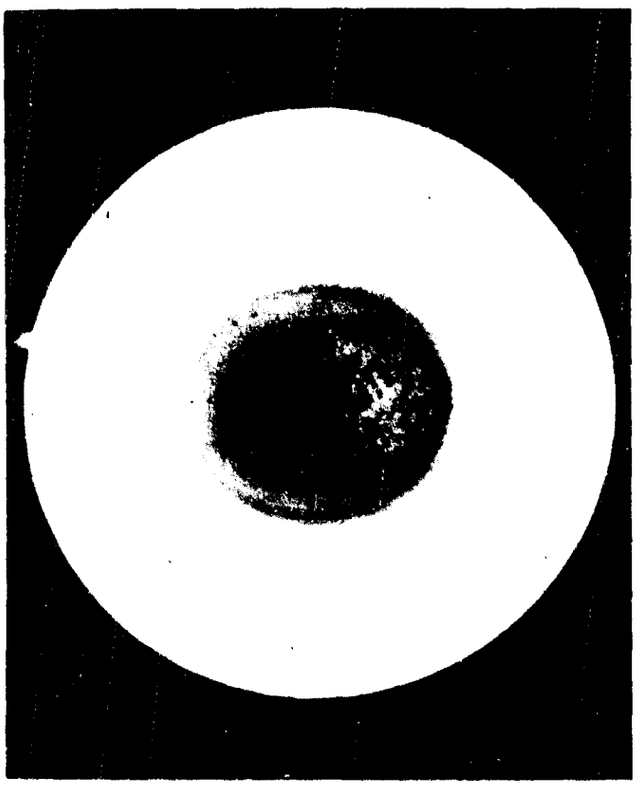

Most of the insoluble solid materials were found to be agglomerates of small reddish-orange-to-black spheres. Some of these were as large as 30 microns in diameter (see Figure 2.11). From their x-ray diffraction pattern, the spheres were identified as being composed of dicalcium ferrite. In these particular samples, only about 15 percent of the activity diffused into the reagent films; the remainder was associated with the solids. The iron came from the large steel barge, and the calcium came from the coral sand used as ballast in the barge.

For these sea water fallout particles, the association of the results of the analyses with possible high-temperature reactions is not quite as straightforward as for the completely solid particles from the other types of detonations. Because of the presence of water, the droplet or particle can change in size. Perhaps changes in the relative amounts of various chemical constituents also occur during the fall of the droplet through the atmosphere. These changes are due to evaporation of water in the drop or to the condensation of atmospheric water vapor as well as to a continual process of accretion of neighboring particles.

Certainly a large amount of sea water would be vaporized initially along with the fission-product elements and the solid materials of the bomb structure (including the barge and ballast in the test shots). The iron and calcium oxide vapors condense, to form the small calcium ferrite particles, in much the same way as was observed in the fallout from the coral surface and tower detonations. These oxides and some of the more refractory fission-product oxides would condense first, at the higher temperatures. The next substances to condense are the sodium chloride and the less refractory fission products (oxides, hydroxides, or chlorides). And finally, at temperatures around 100°C, the water vapor condenses. It is likely that the first particles to be formed serve as nuclei or surfaces upon which the remaining vapor condenses, although this may not be the only process involved. The same final particle could be formed by separate condensation of the various substances and by particle growth by impaction, especially when the water drops are present in liquid form and in high concentration.

The water content of the final particle would depend on the humidity and temperature conditions of the atmosphere through which it falls. While the final water content of the particle would be determined to a large degree by these conditions in the latest part of their fall trajectory near the earth, the particles carried to great altitudes would fall through air layers at temperatures less than 0°C. In these layers, the particles would be solid, and the time that they would remain in the solid state from a large yield detonation would be a large fraction of

Figure 2.11
ELECTRONMICROGRAPH OF THE RADIOACTIVE SOLIDS IN THE LIQUID FALLOUT PARTICLES FROM A LARGE-YIELD BARGE SHOT AT THE ENIWETOK PROVING GROUND. THIS AGGLOMERATION OF VERY SMALL SPHERES, EACH FORMED FROM THE CONDENSATION OF THE VAPORIZED BARGE AND BALLAST MATERIALS, IS COMPOSED LARGELY OF DICALCIUM FERRITE

their total fall time. The loss and/or gain in water content during the fall would result in corresponding changes in particle size and density as well as in fall velocity of the particle.

2.2.7 Conclusions Regarding Fallout Particle Formation Processes

The consistent inferences of the data, with regard to the formation of the fallout particles in the cooling fireball, are:

1. The vapor-condensation of small particles begins at the highest temperature at which a macroscopic liquid phase can exist in equilibrium with its saturated vapor. The substance forming this initial liquid phase is always a nonradioactive material such as the metal oxides from the structural compounds of the weapon and/or the decomposition products of the soils. These substances are the ones, nearest the point of detonation, whose vapors are intimately mixed with the fission-product gas atoms. Some of the fission product atoms or molecules condense to form a dilute solution in these particles.

2. Heated soil (and tower) materials are drawn into the fireball as it rises; some of these form particles from the disintegration of a bulky layer of liquid material or are otherwise melted before they enter the cooling fireball. Certain other particles are melted after they enter the fireball, some are only partially melted, and some are not melted at all. The degree of heat treatment received by the various types of particles depends upon the time the particle entered the fireball, its trajectory through the hot gases, the temperatures along that trajectory, and the particle's velocity.

3. The larger of the melted particles collide with and dissolve the small vapor-condensed particles, thus acquiring the radioactive elements they contain.

4. Radioactive elements that remain in the gaseous state during the time these melted particles exist--that is, when the fireball temperature is between the melting and boiling points of the particles--vapor-condense directly onto the particle surfaces to form dilute solutions of the mutually-soluble oxides or compounds. The elements may solidify as separate phases in the particles if the concentration is sufficiently large or remain essentially as an impurity site in the crystal or glass phase of the larger melted particles.

5. The latest solid particles to arrive in the fireball collide with and scavenge some of the remaining small particles, which then remain on the surface of the larger (unmelted) particles. Since these solid particles collect on their surfaces other particles as large as 10 microns in diameter, they can also vapor-condense on their surfaces the more volatile of the radioactive atoms not previously condensed into the liquid particles. And, since some of the fission products are rare gas elements, this latter type of condensation proceeds as long as the particles and gas atoms remain together.

2.3 Solubility Properties of Fallout

The solubility of various radionuclides from local fallout particles (silicate type) is a general indicator of how much of the radionuclides had condensed on the exterior of the particles in the second period of condensation. The solubility properties can be inferred directly from solubility measurements and indirectly from the uptake of the radionuclides in biological systems.

The solubility in water is somewhat similar to the solubility process for incorporation of radioelements by plants in that the dissolution takes place in near-neutral water systems. The major difference in the two systems is the presence of the soil as an ion-exchanger for the plant uptake system.

The solubility in acids is similar to the solubility process in which the fallout particles are ingested by animals through consumption of externally contaminated plant parts, since the stomach fluids are acidic.

Unfortunately, most of the available radionuclide solubility data is reported in terms of the fraction of the gross activity (as beta or gamma count-rates) that is removed from the fallout particles in water or dilute acids. Nishita and Larson,[13] for example, report solubilities for larger particles with diameters from about 300 to 900 microns that range from 0.3 to 1.2 percent of the beta activity removed by water and from 2 to 10 percent removed by 0.1N-HCl. However, the liquid volumes and times of operation are not reported. Solubility data on size-separated soil-plus-fallout samples from tower-mounted detonations, as reported by Nishita and Larson, are summarized in Table 2.1; low activity levels and variation in soil type likely contributed to the scatter in the data. However, the authors conclude that the smaller particle size fractions showed the greater solubility.

Table 2.1

PERCENT OF GROSS BETA COUNT-RATE REMOVED FROM SOIL-PLUS-FALLOUT SAMPLES COLLECTED AT DIFFERENT LOCATIONS AND ARRANGED BY AVERAGE PARTICLE SIZE[13]

Average Particle Diameter (microns)	Tesla	Apple I	Met	Apple II
	A. Water			
2.5	1.9	0.9(?)[b]	3.0	4.2
66	7.6	0.0(?)	-	2.8
106	1.8	-	0.0(?)	-
151	0.1	44	-	0.5
214	-	-	0.2	-
275	-	18	-	-
325	-	0.2	-	-
670	-	-	-	33 (?)
	B. 0.1N-HCl			
2.5	19	25	19	28
66	30	41	-	14
106	54 (?)	-	4.4	-
151	1.5	56	-	4.0
214	-	-	11	-
275	-	32	-	-
325	-	0.7	-	-
670	-	-	-	2.4

a Tesla; W = 7KT on 300' Tower
Apple I; W = 14KT on 500' Tower
Met; W = 22KT on 400' Tower
Apple II; W = 29KT on 500' Tower

b Question inserted where the relative solubilities indicate a large divergence from the set average.

Other direct measurements of the gross solubility of fallout collected at the Nevada Test Site, for several different detonation conditions, as summarized by Larson and Neel,[14] are shown in Table 2.2. Although the average times after detonation for the data are not given (presumed to be about 2 weeks), the general magnitudes of the fractions of the activity which were soluble indicate the nuclides in the fallout from the balloon-mounted (i.e. air-burst) detonations to be most soluble. The higher solubility in water especially suggests that larger amounts of the radionuclides were condensed on the surfaces of the particles in the balloon-mounted detonations. The very high solubilities in acid for these particles were probably due to dissolution of the primary iron oxide or alumina particles.

It may be noted that the solubility in both water and acid for the larger particles in the fallout from the balloon-supported detonations is greater than for the smaller particles. This suggests a very high degree of surface condensation of the radionuclides at late times since a significant fraction of the larger particles was melted grains of soil. The averaged solubility of the activity on the particles from the tower-mounted detonations, on the other hand, decreased with increasing particle size. Fused soil fallout particles with diameters of 200 to 2,000 microns from low-tower detonations often have negligible solubilities, in water or even in strong acids.[15]

Gross solubility data for small fallout particles lodged on foliage after some tower detonations, reported by Romney and co-workers,[16] are summarized in Table 2.3. Since the data do not indicate a consistent trend in solubility with distance from ground zero (indicating that the particle sizes retained by the foliage was about the same at all locations), the average fractional solubilities were calculated for each shot. These averages agree fairly well with the solubilities given in Table 2.1 for the particles with a 2.5 micron average diameter.

The major contributing radioelements found in the tissue of rabbits and rodents taken from areas near the Nevada Test Site on which small fallout particles deposited within the first day after a test detonation include iodine, strontium, yttrium, ruthenium, cesium, barium, and cerium.[14,17,18,19] The tissue concentrations increased with distance from shot point up to a maximum and then decreased again. The maximum tissue concentrations generally occurred at locations where the fallout arrival time was about 2 to 3 hours after detonation. These data indicate that the fraction of the radioelements on the exterior of the particles available for uptake increased with decreasing particle size more rapidly than the total amount of fallout deposited decreased with distance, up to some distance. At farther distances, the decrease

Table 2.2

GROSS SOLUBILITY OF ACTIVITY FROM SMALL FALLOUT PARTICLES

Type of Detonation	Percent Activity Soluble[a] in H_2O	Percent Activity Soluble[a] in 0.1N HCl	Particle Size (microns)
Underground	5.4	25	0-44
Tower-Mounted	2	14 to 36	0-44
	1	5	44-ca 100
Balloon-Supported	14	60	0-44
	31	90	44-ca 100

a Based on beta count-rate measurements (presumably at about 2 weeks after detonation).

Table 2.3

GROSS SOLUBILITY OF ACTIVITY FROM SMALL FALLOUT PARTICLES LODGED ON PLANT FOLIAGE

Plant Type	Distance from Ground Zero (miles)	Fraction Dissolved[a] in 0.1N HCL
1. Shot Apple I (14 KT on 500 ft Tower)		
Artemisia (Sagebrush)	12	0.20
Ephedra (Mormon tea bush)	40	0.27
Ephedra (Mormon tea bush)	80	0.15
Juniperus (Juniper)	165	0.32
	Average:	0.24
2. Shot Met (22 KT on 400 ft Tower)		
Larrea (Creosote bush)	20	0.26
Larrea (Creosote bush)	58	0.08
Medicago (Alfalfa)	140	0.14
	Average:	0.16
3. Shot Apple II (29 KT on 500 ft Tower)		
Triticum (wheat)	7	0.19
Triticum (wheat)	40	0.17
Triticum (wheat)	106	0.35
	Average:	0.24

a Based on beta count-rate measurements

in the deposit level predominated, and the amount of uptake also decreased with downwind distance.

Radioiodine was found to be 80 to 90 percent of the activity in the thyroid tissue of native rodents.[14] The radioelements found in the bone tissue of jack rabbits at about 20 days after a tower shot are listed in Table 2.4 in which a few of the data given by Larson and Neel[14] have been converted to number of atoms and approximate fission equivalents taken up and deposited in the bone tissue. The relatively low uptake factor of yttrium, ruthenium, and cerium (last column of the table) is probably due to both a lower solubility in the rabbit digestive tract and lower retention of these elements in the bone tissue of rabbits.

The main point of the animal assimilation data is that the listed radioelements were dissolved by the acidic digestive tract fluids from small fallout particles that pass through the gut. Other radioelements in fallout, but not listed, presumably were not dissolved in appreciable or significant amounts. The listed elements are those expected to be depleted in the larger fallout particles, and enriched in the smaller fallout particles, relative to the other refractory type fission-product elements, as well as being condensed on the surfaces of these smaller particles so that they are biologically available to plants and animals.

2.4 Radioactive Elements in Fallout

2.4.1 Sources of Radioactive Elements

The amount of each radioactive element that is actually found in fallout, relative to some standard of measure, depends on seven main factors:

1. The original fission yields, that is, the relative abundance of the fission products

2. The capture of neutrons by the fission products themselves

3. The degree to which each fission product condenses into or onto the carrier particles

4. The neutron emissions in the decay chain

5. The capture of neutrons by bomb structural materials

Table 2.4

RELATIVE RADIOELEMENT CONCENTRATIONS IN JACK RABBIT BONE TISSUE
AT ABOUT 20 DAYS AFTER DETONATION OF SHOT SMOKY, OPERATION PLUMBBOB, IN 1957

Radionuclide	A(20 days) (d/m)/ (gm bone)	N(20 days) (atoms/ gm bone)	N_f(21 days)[a] (atoms)/ fission)	1 - r_j(A)[b] (availability factor)	A_o (fissions/ gm bone)	N_f[c] (retention factor)
Sr-89	200	2.2×10^7	0.0309	0.989	7.2×10^8	1.0
(Sr-91)Y-91	35	4.1×10^6	0.0420	0.838	1.2×10^8	0.2
Ru-103(Ru-106)	4.5	3.7×10^5	0.0235	0.572	0.28×10^8	0.04
Cs-137	1.7	4.8×10^7	0.0577	0.993	8.38×10^8	1.2
Ba-140	700	1.9×10^7	0.0195	0.791	12.3×10^8	1.7
Ce-141(Ce-144)	4.0	2.7×10^5	0.0384	0.133	0.53×10^8	0.07

a For fission products from thermal fission of U-235 (see Reference 20)

b r_j(A) taken from the calculations of Chapter 4 for the 1-MT surface burst without correction for yield and type of detonation

c Relative retention factor assuming value of 1.0 for Sr

6. The capture of neutrons by environmental materials

7. The radiochemical standards used in measuring the relative abundances of the fission products

The relative abundance of each fission-product element originally produced at detonation depends on the fissile material used, i.e. whether the material is U-235, U-238, Pu-239, or some other nuclide. The fission-chain yields also depend on the energy spectrum of the incident neutrons.

Neutron capture by the fission-product elements should result in a general shift of the whole fission-yield curve to the higher-mass numbers. This should cause a decrease in the yields of the elements of both mass groups that have the smaller mass numbers (the left sides of the peaks) and an increase in the yields of the elements of both mass groups that have larger mass numbers. In the yields of the elements in the peaks, relatively little change results except for those elements that have extremely high neutron-capture cross sections. The subject is not discussed further because of insufficient data.

During the decay process, neutron emission results in a product nuclide that has a mass number that is a single unit less than its parent. This chain "shift" can be accounted for if the decay scheme of the radionuclide is known. For many of the short-lived radionuclides, however, there is insufficient data presently available for giving further consideration to decay by neutron emission.

Many of the neutrons that are produced in both the fission and fusion processes are captured by bomb or warhead structural materials such as U-238, iron, aluminum, and other metals. The relative induced yields of radionuclides from these materials depend upon the fission to fusion yield ratios of the weapon, the total weapon yield, and the relative amounts of the different materials present.

The capture of neutrons that "escape" from the weapon materials during the detonation by air and other environmental substances (such as soil) produces additional amounts of radioactivity. The activation of sodium and manganese in soils that becomes part of local fallout from surface detonations has been previously mentioned. Neutron capture by both nitrogen and oxygen in air leads to the production of carbon-14; the latter, of course, is not found to any significant amount in the local fallout particles.

The experimental measure of the relative yields of different radionuclides in fallout is most often given as an "R" factor, or "R" value, that is relative to the fission yields in the thermal-neutron fission of U-235 and of a selected radionuclide. The most commonly selected radionuclide for comparison is Mo-99. However, a radiochemical assay of a fallout sample that gives an R value different from unity does not necessarily mean that the nuclide in question has, in fact, been fractionated with respect to some other nuclide or element. The true initial fission yields must be known, both to correct the observed assay data and to determine whether fractionation has, in fact, occurred.

2.4.2 Fission Product and Neutron Yields in Nuclear Explosions

One major factor that determines the amount of a fission product that condenses with the carrier up to a given time and temperature is the amount of that element present in each of the mass chains. In this section, data on the fission-mass yields are summarized, and estimates of undetermined yields are presented.

Available mass chain yield data and estimates of unmeasured yields are summarized in Table 2.5 for the fission of U-235, U-238, and Pu-239. The bulk of the data are taken from the summaries by Katcoff;[21,22] other references are included in the table.

The yield curve for thermal neutron fission of U-235 gives an average value of 2.5 neutrons per fission. For fission-spectrum neutron fission of U-238, an average value of 3.1 neutrons per fission is obtained. These two values, together with the referenced data in Table 2.5, were used to derive the chain yield curve for the 8-Mev neutron fission of U-238. The yields for instantaneous fission of Pu-239 were taken from the calculations of Weaver et al.

The fission processes with fission spectrum neutrons generally yield about 3 neutrons per fission, and the 8-Mev fission chain yields, as listed, indicate a production of about 4 neutrons per fission.

Comparison of the cumulative chain yields at the two peaks (A = 90 to 100 and A = 131 to 144) for these types of fission indicates that no very large differences in the gross decay rates of the fission products from the three fissile nuclides should be expected. The mass-chain yields for fission-neutron fission of Pu-239 appear to differ most from the yields of the thermal-neutron fission of U-235; for mass numbers such as 140 and 95, whose radioisotopes may contribute more than 80 percent of

Table 2.5

CUMULATIVE MASS-CHAIN YIELDS OF FISSION PRODUCTS
(VALUES ARE IN PERCENT OF FISSIONS)

	U-235		U-238			Pu-239	
Mass Number	Thermal Neutrons	Fission Neutrons	Fission Neutrons	8-Mev Neutrons	"Thermonuclear Fission"	Thermal Neutrons	Fission Neutrons
72	1.6×10^{-5}	4.6×10^{-4}	5.0×10^{-6}	-	-	1.2×10^{-4}	-
73	1.1×10^{-4}	0.0012	3.7×10^{-5}	-	-	2.5×10^{-4}	-
74	3.2×10^{-4}	0.0034	1.1×10^{-4}	0.001	-	6.2×10^{-4}	-
75	8.8×10^{-4}	0.0062	8.3×10^{-4}	0.0040	-	0.0014	0.0017
76	0.0029	0.012	0.0012	0.0078	-	0.0038	0.0038
77	0.0083	0.023	0.0038	0.014	0.0105	0.0014	0.019
78	0.021	0.048	0.0095	0.026	0.0202	0.012	0.036
79	0.041	0.096	0.019	0.053	0.0366	0.025	0.066
80	0.077	0.19	0.045	0.096	0.0697	0.048	0.11
81	0.14	0.21	0.083	0.18	0.105	0.096	0.17
82	0.29	0.50	0.20	0.35	0.224	0.17	0.26
83	0.544	0.80	0.40	0.66	0.501	0.29	0.38
84	1.00	1.3	0.85	1.02	0.782	0.47	0.52
85	1.30	1.85	0.80	1.45	1.10	0.54	0.70
86	2.02	2.5	1.38	1.9	1.45	0.76	0.91
87	2.94	3.3	1.90	2.25	1.86	0.91	1.15
88	3.92	4.2	2.45	2.7	2.27	1.40	1.43
89	4.79	5.1	2.9	3.17	2.68	1.71	1.74
90	5.77	5.8	3.2	3.7	3.09	2.24	2.23
91	5.84	5.85	3.6	4.3	3.67	2.89	2.44
92	6.03	6.0	4.1	4.8	4.11	3.09	2.89
93	6.45	6.4	4.85	5.2	4.71	3.96	3.33
94	6.40	6.4	5.3	5.45	5.04	4.46	3.80
95	6.27	6.3	5.7	5.6	5.10	4.99	4.31
96	6.33	6.3	5.8	5.7	5.22	5.14	4.82
97	6.09	6.1	5.7	5.64	5.32	5.59	5.28
98	5.78	5.8	5.7	5.6	5.40	5.81	5.75
99	6.06	6.1	6.3	6.2	5.48	6.09	6.10
100	6.30	6.7	6.1	6.4	5.43	7.06	6.86
101	5.0	5.3	5.5	6.5	5.32	5.87	6.75

Table 2.5 (continued)

CUMULATIVE MASS-CHAIN YIELDS OF FISSION PRODUCTS
(VALUES ARE IN PERCENT OF FISSIONS)

	U-235		U-238			Pu-239	
Mass Number	Thermal Neutrons	Fission Neutrons	Fission Neutrons	8-Mev Neutrons	"Thermonuclear Fission"	Thermal Neutrons	Fission Neutrons
102	4.1	2.9	5.6	5.9	5.11	5.96	6.65
103	3.0	1.7	6.6	5.0	4.90	5.60	6.35
104	1.8	0.95	5.4	3.2	4.33	5.88	5.86
105	0.90	0.54	3.9	2.2	3.89	5.18	5.24
106	0.38	0.30	2.7	1.5	3.35	4.54	4.64
107	0.19	0.17	1.35	1.0	2.76	3.44	3.95
108	0.085	0.095	0.67	0.70	2.21	2.55	3.12
109	0.039	0.053	0.32	0.48	1.55	1.38	2.03
110	0.020	0.030	0.15	0.33	0.794	0.75	0.76
111	0.015	0.022	0.073	0.23	0.422	0.23	0.32
112	0.013	0.020	0.046	0.19	0.300	0.12	0.14
113	0.012	0.018	0.043	0.17	0.260	0.12	0.10
114	0.011	0.017	0.041	0.16	0.260	0.055	0.081
115	0.0104	0.017	0.040	0.15	0.250	0.041	0.068
116	0.010	0.017	0.039	0.14	0.249	0.037	0.066
117	0.010	0.017	0.039	0.14	0.245	0.036	0.064
118	0.010	0.017	0.040	0.14	0.241	0.035	0.064
119	0.011	0.017	0.041	0.14	0.245	0.036	0.064
120	0.011	0.018	0.042	0.15	0.248	0.037	0.064
121	0.012	0.020	0.044	0.16	0.250	0.043	0.065
122	0.013	0.022	0.046	0.17	0.252	0.047	0.068
123	0.015	0.030	0.050	0.19	0.260	0.056	0.081
124	0.017	0.053	0.055	0.23	0.301	0.070	0.099
125	0.021	0.095	0.072	0.33	0.421	0.095	0.13
126	0.058	0.17	0.175	0.48	0.790	0.16	0.18
127	0.145	0.30	0.39	0.70	1.56	0.38	0.35
128	0.37	0.54	0.77	1.0	2.21	0.85	1.67
129	0.90	0.95	1.45	1.5	2.78	1.69	2.98
130	2.0	1.7	2.5	2.2	3.34	2.69	3.86
131	2.88	2.9	3.2	3.2	3.90	3.76	4.57

Table 2.5 (continued)

CUMULATIVE MASS-CHAIN YIELDS OF FISSION PRODUCTS
(VALUES ARE IN PERCENT OF FISSIONS)

	U-235		U-238			Pu-239	
Mass Number	Thermal Neutrons	Fission Neutrons	Fission Neutrons	8-Mev Neutrons	"Thermonuclear Fission"	Thermal Neutrons	Fission Neutrons
132	4.31	4.3	4.7	4.4	4.34	5.21	5.20
133	6.48	6.1	5.5	5.4	4.91	6.85	5.74
134	7.80	7.3	6.6	6.5	5.12	7.44	6.22
135	6.40	6.3	6.0	5.9	5.32	7.08	6.56
136	6.36	6.4	5.9	5.8	5.42	6.58	6.85
137	6.05	6.0	6.2	5.85	5.46	6.59	6.90
138	5.74	5.7	6.4	5.9	5.42	6.29	6.10
139	6.34	6.4	6.5	6.0	5.32	5.84	5.64
140	6.44	6.4	5.7	5.6	5.22	5.60	5.08
141	6.30	6.3	5.7	5.5	5.10	5.31	4.51
142	5.85	5.9	5.7	5.4	4.98	4.98	4.06
143	5.87	5.8	5.5	4.97	4.72	4.54	3.61
144	5.67	5.1	4.9	4.3	4.11	3.88	3.20
145	3.95	4.2	3.7	3.7	3.64	3.09	2.78
146	3.07	3.3	3.1	3.17	3.09	2.60	2.42
147	2.38	2.5	2.6	2.7	2.67	2.06	2.05
148	1.70	1.85	2.0	2.27	2.27	1.69	1.71
149	1.13	1.3	1.45	1.9	1.87	1.31	1.40
150	0.67	0.80	1.05	1.45	1.46	1.00	1.12
151	0.45	0.50	0.74	1.02	1.11	0.80	0.88
152	0.285	0.31	0.50	0.66	0.781	0.61	0.68
153	0.15	0.19	0.32	0.41	0.497	0.37	0.49
154	0.077	0.096	0.19	0.25	0.225	0.29	0.36
155	0.033	0.048	0.11	0.15	0.105	0.23	0.25
156	0.014	0.023	0.066	0.092	0.0628	0.11	0.18
157	0.0078	0.012	0.034	0.057	0.0368	0.076	0.11
158	0.002	0.0062	0.016	0.032	0.0202	0.042	0.072
159	0.00107	0.0034	0.0090	0.017	0.0106	0.021	0.046
160	3.5×10^{-4}	0.0012	0.0036	0.0085	-	0.0098	0.026
161	7.6×10^{-5}	4.6×10^{-4}	9.4×10^{-4}	0.0044	-	0.0039	0.014

Table 2.5 (concluded)

CUMULATIVE MASS-CHAIN YIELDS OF FISSION PRODUCTS
(VALUES ARE IN PERCENT OF FISSION)

Table 2.5 References:

1. Katcoff, Seymour, "Fission-Product Yields from U, Th and Pu," Nucleonics, Vol. 16, No. 4, p. 78-85 (1958); Vol. 18, No. 11, p. 201 (1960)

2. Bunny, L. R., E. M. Scadden, J. O. Abriam, and N. E. Ballou, Radiochemical Studies of the Fast Neutron Fission of U-235 and U-238, Second U.N. International Conference on the Peaceful Uses of Atomic Energy, A/Conf. 15/P/643, USA, June 1958

3. Ford, G. P., and J. S. Gilmore et al, Fission Yields, LADC-3083,

4. Bunney, L. R., E. M. Scadden, J. O. Abriam, and N. E. Ballou, Fission Yields in Neutron Fission of Pu-239, USNRDL-TR-268, 1958

5. Weaver, L. E., P. O. Strom, and P. A. Killeen, Estimated Total Chain and Independent Fission Yields for Several Neutron-Induced Fission Processes, USNRDL-TR-633, 1963

6. Crocker, G. R., Estimates of Fission Product Yields of a Thermonuclear Explosion, USNRDL-TR-642, April 1963

the total gamma radiation at specific times after fission, the ratio of the Pu-239 to U-238 yields is 0.79 for mass number 140 and 0.69 for mass number 95. The yield of mass number 90 is significantly lower for U-238 (8-Mev neutrons) and Pu-239 (fission neutrons) relative to the yield for thermal fission of U-235; the yield ratios are 0.64 and 0.39, respectively.

The yields of mass number 137 are all more nearly alike. The largest chain yield differences occur for mass chains between the two yield peaks and for the nuclides that appear at the highest and lowest mass numbers. But even for U-238 fission (8-Mev neutrons), where the yields of the mass numbers near 118 are more than a factor of ten larger than the yield for U-235 fission (thermal neutrons), the contribution of these "valley" elements is a small fraction of the total radioactivity of the fission products.

To use the mass chain-yield values in computations of the amount of each element that is condensed to form fallout and in calculating the gross decay rate of the mixture requires some estimate of the independent yields calculated by Bolles and Ballou[19] for thermal-neutron fission of U-235 are converted to fractional chain yields so that they may be applied directly to all the cumulative mass-chain yields for each type of fission.

Although it appears that Glendenin's symmetrical charge-distribution[24] curve is generally applicable for all fissile nuclides in low energy neutron fission, it has been shown[25] that the most probably charge, Z_p, (for a given mass distribution) shifts toward stability with increasing neutron energy. That is, the higher fractional yields appear farther to the right (toward a higher Z number) in any decay chain. Pappas[26] used a discontinuous function for Z_p and considered the primary fragments before neutron boil-off; however, Wahl[27] has shown empirically that the Z_p function in thermal fission of U-235 is continuous, as was originally postulated by Glendenin et al.[28] Herrington[29] proposes two charge-distribution curves--one for the even-neutron nuclides and another, showing a lower yield, for the odd-neutron nuclides.

The recent tabulation by Weaver et al[23] of the total and independent fission yields for use in updating and extending the Bolles-Ballou computation again utilized Glendenin's symmetrical charge distribution curve. The values for Z_p, however, were taken from Coryell[30] and were discontinuous in the neighborhood of shell and subshell closures A correction to Z_p was also given by Coryell for conditions other than thermal-neutron fission of U-235.

It is clear that there is no unequivocal choice among methods for estimating the independent yields of the chain members, even for thermal-neutron fission of U-235. For the independent yields of higher-energy fission, the experimental data are rarer yet. It is therefore assumed in the calculations following that the fractional independent yields for thermal fission of U-235 calculated by Bolles and Ballou on Glendenin's postulate are not too inappropriate for any kind of fission with low-energy neutrons. The assumption is borne out reasonably well by Weaver's results. Additional total yield information due to Katcoff[22] in general supports the estimates made earlier in Table 2.5.

The total energy released in the fission process can be calculated by using the mass packing-fraction curves for the final stable nuclide in each mass chain, for the fissile nuclide involved, and for the fractional mass-chain yields. The calculated energy releases are:

199 Mev per fission for fission-neutron U-235 fission,
204 Mev per fission for 8-Mev neutron fission of U-238, and
208 Mev per fission for fission-neutron fission of Pu-239.

The corresponding fission energy releases not including the radioactive decay to stable nuclides, obtained from the data reported by Leachman,[31] are 177, 179, and 184 Mev/fission, respectively. The energy released through radioactive decay of all the products thus is about 12 percent of total energy released in these fission processes. With the commonly used conversion factor of 1.0×10^{12} calories per kiloton of TNT,[1] the ratios of the number of fissions to the energy yield in kilotons of TNT for the initial energy releases therefore are: 1.48×10^{23} (U-235, fission-neutrons); 1.46×10^{23} (U-238, 8-Mev neutrons); and 1.42×10^{23} (Pu-239, fission-neutrons). These ratio values should apply to the fission abundances for the weapon yields as generally reported in the available literature.[1]

Many previous computations have been made with a fission-to-yield conversion factor of 1.45×10^{23} fissions per KT, without reference to the type of fissile material.[32] The excess neutrons, produced by the fission process only, are: 0.48 moles per KT for U-235 (fission neutrons), 0.47 moles per KT for U-238 (8-Mev neutrons), and 0.46 moles per KT for Pu-239 (fission neutrons).

The energy and neutron yields that are possible for some thermonuclear reactions can be estimated from the reactions given in ENW (p. 16)[1] as well as from other similar fusion reactions of light elements. Most of these combinations give reaction energies in the range of 10 to 25 Mev and neutron yields of between zero and 2 for each reaction. Thus, for

the energy release and the neutron yields of thermonuclear rea tions, a reasonable estimate seems to be that about 0.3 KT of energy per mole of reactant is released and about 2.5 moles of neutrons per KT are produced.

In all thermonuclear weapons, the total yield of the explosion is the sum of the energy released by both the fission and the fusion processes. However, the amount of radioactive fission products produced depends only on the fission yield. Thus the ratio of fission to total yield is an important quantity since the concentration of the fission products in the fallout is directly proportional to the ratio of the fission yield to the total weapon yield. For example, if the fission and fusion yields of a thermonuclear weapon are equal, the radiation from the fallout would be about half that of a pure fission weapon of the same yield.

The number of neutrons produced is also of interest in fallout. Since all the neutrons released are captured by some nearby atom, a considerable amount of additional radioactivity may result. It may be noted that in the fission of U-238 the number of radioactive product elements produced is 0.47 moles/KT. If all of the excess neutrons were captured by some substance to produce a radioactive product, the total initial radioactive yield would be 1.17 moles/KT. In the same situation, but for a pure thermonuclear yield, the neutron activations alone would amount to about 2.5 moles/KT.

Thus, theoretically, a pure thermonuclear (or so-called "clean") weapon could have a radiological capability twice that of a pure fission weapon. But it would be a rare occurrence that this capability would be realized because many of the naturally occurring elements that are in large abundance (such as hydrogen, silicon, oxygen, and aluminum) can capture neutrons to produce either another stable nuclide or a very short-lived radionuclide. On the other hand, if a thermonuclear explosion took place where such elements as sodium (salt), manganese, cobalt, and so on were concentrated in large quantities, the radioactive yield of these elements could be expected to be high.

2.4.3 Radionuclide Fractionation

Only a limited amount of unclassified information is available from radiochemical analyses of fallout particles. The first information of this kind was reported by Kimura[33] et al, who presented analyses of the fallout from Shot Bravo, detonated on March 1, 1954. The fallout

Table 2.6

CALCULATION OF RELATIVE ACTIVITY RATIOS FROM KIMURA'S DATA ON CORAL FALLOUT[33]

Nuclide	Half-Life	Percent of Total Activity on D+25	Percent of Fission Product Activity on D+25	Percent of Activity for U-238 Fission on D+25	Ratio ($\frac{\%\ \text{Observed}}{\%\ \text{for U-238}}$)	Adjusted Percent of Fission Products in Fallout	Fractionation Number[b]
Sr-89	53d	1±0.5	1.25	4.01	0.31	.90	0.22
Sr-90	28y	0.02±0.01	0.025	0.053	0.47	0.018	0.34
Y-90	61h	0.02±0.01	0.025	0.053	0.47	0.018	0.34
Y-91	57d	8±3	10.0	5.89	1.70[a]	7.22	(1.0)
Z-95	65d	5±2	6.25	6.94	0.90[a]	4.51	(1.0)
Nb-95	35d	3±1	3.75	3.06	1.23[a]	2.71	(1.0)
Ba-140	12.8d	5±1	6.25	11.92	0.52	4.51	0.38
La-140	40h	6±1	7.50	13.69	0.55	5.41	0.40
Ce-141	31d	7±5	8.75	10.55	0.83[a]	6.31	(1.0)
Ce-144	282d	2±1	2.50	1.49	1.68[a]	1.80	(1.0)
Pr-143	13.7d	16±5	20.0	12.02	1.66[a]	14.4	(1.0)
Pr-144	17.5m	2±1	2.5	1.49	1.68[a]	1.80	(1.0)
Nd-147	11.3d	9±4	11.25	5.46	2.06[a]	8.12	(1.0)
U-237	6.75d	20±10	-	-	-	-	-
Pu-239	24,360y	$(4\pm2)\times10^{-4}$	-	-	-	-	-
		Sum	82.55				
		Missing	17.45				

a Nuclides with these ratios are assumed to be in correct relative abundance; the ratio of their sums (65.0% of FP activity observed, 46.9% of FP activity for normal U-238 mixture) is 0.72.

b The values of the fractionation number are calculated from the ratios of the values of Column 6 to those of Column 4, except for the elements which are assumed to have values of unity.

for these analyses contaminated the Japanese boat No. 5 Fukuryu Maru. Some of the particles, called ashes or dust because of the white color of calcium carbonate or hydroxide, were collected by the crew of the ship who carried the material back to the Japanese mainland where the analyses were made.

In the report, Kimura chose to refer his data to the thermal-neutron fission of Pu-239. The data were reanalyzed on the basis of 8-Mev neutron fission of U-238 because of the reported high abundance of the nuclide, U-237, presumably produced by a (n, 2n) reaction on U-238. In this instance, the Pu-239 was presumably produced by a (n, γ) reaction on U-238 in which the initial product, U-239, had, to a great degree, decayed to Np-239 and then to Pu-239 by the time of the analyses. Kimura's data, compared with the calculated activities for U-238 fission at D + 25 (25 days after detonation), are summarized in Table 2.6.

The data summary shows the depletion of the nuclides Sr-89, Sr-90, Y-90, Ba-140, and La-140, all of which are daughter products of rare gas precursors. Further analysis[34] of the data[33] also revealed that fallout was relatively depleted in the concentrations of the radioelements Ru, Rh, Te, I, and Cs. The radiochemical data[33] also indicated neutron capture yields of at least 0.3 atoms per fission for U-239 and 0.15 atoms/fission for U-237.

The second set of unclassified data on the radiochemical content of radioactive particles was reported by Mackin and co-workers at NRDL.[35] The sample particles were obtained from detonations on coral islands at the Eniwetok Proving Grounds in 1956. In this case, analyses are made for only a few radionuclides: Mo-99, Sr-89, Ba-140, and Np-239. However, no Np-239 data are reported. In addition, the gross activity of the particles was measured by using a well-crystal (WC) NaI(Tl) scintillation counter and a 4π high-pressure argon gas (at a pressure of 600 psig) gamma ionization chamber.[36]

Many of the particles were weighed so that specific activities could be determined, and some data on gross samples were obtained. The Mo-99 radionuclide was utilized as the "fission" tracer with the assumed yield of 6.1 percent; this yield value is sufficiently close to the yield for the 8-Mev neutron fission of U-238 that no adjustment of the reported values was required. Some of the data are summarized in Table 2.7. The particle type designations "altered" and "unaltered" used by the authors have been changed to "fused" particles and "irregular" particles as the first classification of the particle type since the thin-section analyses showed that most of the irregular particles have been calcined.

Because of analytical requirements, only the more highly radioactive particles were used in the reported analyses. This means that the results are applicable only to a description of the larger particles. However, even with this bias, the results are useful in illustrating the possible range in values of all the measured quantities.

The counting-rate and ion-current measurements were corrected to H + 70 hours before the apparent average ionization rates, WC-rates per fission, ion current per fission, and the specific ionization rate were computed. The decay corrections for the WC measurements were obtained from the reported decay curves for the two types of particles; the ionization rate decay corrections were obtained from unpublished data on particles from the same set of samples. It is quite likely that each particle had its own decay rate, differing to some degree from other particles of the same general type. Therefore, with a single type of decay curve, the corrections to a common time are only approximate.

The variability of the ratio of the ion current to the WC count-rate of the set of particles is the first indication of a gross difference in the relative abundances of the emitted gamma rays of different energies, hence of a variation in the constituent radionuclides. Although the ratios of the two measurements of the gross activity in the fused particles (i.e. spheres or broken spheres) and the irregular particles have values that average 83 x 10^{-17} ma/cpm and 132 x 10^{-17} ma/cpm, respectively, there are overlapping values in each particle group. Perhaps if the number of particles analyzed had been doubled, this ratio as a second particle-type classification or distinction between the two groups, might be less marked. In any case, at H + 70, the activity on or in the irregular particles emitted more high-energy gamma rays than the activity emitted by the fused particles.

The third type of classification of the two types of particles is the comparison count per minute (cpm) per fission of the WC values or the ma per fission ratios. Of the two, the ion current per fission gives the larger differentiation, since it is a more sensitive measure of the total photon energy emitted from the mixture. The unfractionated fission-product mixture from the thermal-neutron fission of U-235 gives an ion current of 39.1 x 10^{-21} ma/fission[37] at H + 70. This should be within a few percent of the ion current per fission for the unfractionated fission products from 8-Mev neutron fission of U-238. The value, 30.9 x 10^{-21} ma/fission, for the fused particles indicates that if Mo-99 is a good fission indicator the relative abundance of many other nuclides in these particles is low. The value, 115.6 x 10^{-21} ma/fission, for the irregular particles indicates that the relative abundance of the other nuclides is high.

Table 2.7

RADIOCHEMICAL DATA ON CORAL TYPE FALLOUT PARTICLES FROM A LARGE YIELD SURFACE DETONATION

Collecting Source	Particle Description	t (H + hrs)	Crystal Well Counter		Gamma Ionization Chamber		f	Particle Weight	Apparent Average Ionization Energy, H + 70	WC/f at H + 70	GIC/f at H + 70	Specific Ionization Rate at H + 70
			Activity (cpm x 10^{-6})	Decay Corrections to H + 70	GIC Assay ma x 10^{11}	Decay Corrections to H + 70 hr	fissions x 10^{-10}	(mg)	(ma/cpm) x 10^{17}	(cpm/f) x 10^{4}	(ma/f) x 10^{21}	(ma/mg) x 10^{11}
A. Fused Particles												
Ship	WI	70	0.217	1.00	26	1.00	0.67		120?	0.324	38.8	
	WS	70	0.0387	1.00	7	1.00		0.0094	181?			745
	YS	70	0.291	1.00	25	1.00	0.72		86	0.404	34.7	
	YS	70	0.527	1.00	41	1.00	1.4		78	0.376	29.3	
	YI	71	0.255	1.01	26	1.01	0.80		102	0.322	32.8	
	WI	73	0.237	1.02	19	1.05	0.49		83	0.493	40.7	
	YS	73	0.210	1.02	19	1.05	0.79		93	0.271	25.2	
	WS	74	0.172	1.04	16	1.07			96			
Island	YI	100	8.80	1.39	497	1.55	22.0	2.196	63	0.556	35.0	351
	YS	104	1.17	1.45	108	1.64			104			
	S	105	19.3	1.46	1,320	1.65	75.0	2.246	77	0.376	29.0	970
	WS	119	6.75	1.68	511	1.95	17.0	3.302	88	0.667	58.6	302
Barge	YS	239	17.5	4.60	1,090	5.60		6.90	76			884
	YS	239	37.8	4.60	3,300	5.60		17.3	106			1,070
	YS	239	36.6	4.60	2,720	5.60		8.70	90			1,750
	S	239	6.30	4.60	244	5.60			47?			
	S	239	16.7	4.60	895	5.60			65			
	S	239	24.3	4.60	1,400	5.60		7.10	70			1,100
	S	239	9.05	4.60	490	5.60		2.50	66			1,100
	S	239	2.63	4.60	164	5.60	49.0	1.73	76	0.247	18.8	531
	YS	239	6.72	4.60	465	5.60		5.10	84			510
	YI	239	28.0	4.60	1,720	5.60		25.8	75			373
	YS	532,481	2.70	21.2	360	14.2	190.0	2.76	86	0.311	26.9	1,850
	WS	532,481	1.64	21.2	199	14.2	150.0	1.76	81	0.232	18.8	1,610
B. Irregular Particles												
Ship	WI	70	0.358	1.00	50	1.00	0.67		140	0.534	74.6	
	WI	72,71	0.0411	1.02	2	1.02			49?			
	WI	75,74	0.266	1.04	29	1.04	0.34		109	0.813	88.6	
	WI	75,74	0.0173	1.04	3	1.04			173			
Island	GI	98	3.61	1.30	432	1.38	6.4	16.440	127	0.733	93.1	36.3
	I	99	1.71	1.31	183	1.39		6.110	114			41.6
	WI	99	3.52	1.31	172	1.39	1.9	8.600	52?	2.43?	126	27.8
	WI	100	2.45	1.32	316	1.40	3.7	8.170	135	0.685	120	54.2
	WI	103	0.0361	1.36	3	1.44		3.530	88?			1.22x
	I	103	3.33	1.36	257	1.44	2.6	3.200	82?	1.74	142	116
	WI	104,103	1.12	1.38	141	1.44	1.0	4.123	131	1.54	203	49.3
	I	104	0.0342	1.38	4	1.46		0.171	124			34.1
	GI	105	0.751	1.39	95	1.47	0.64	0.920	134	1.63	218	152
	GI	105	0.208	1.39	24	1.47		1.883	122			18.7
	WI	105	0.830	1.39	116	1.47	0.87	0.872	148	1.33	196	196
	WI	119	0.114	1.58	16	1.67		0.393	148			68.0
	WI	119	0.110	1.58	12	1.67		0.668	115			30.0
	GI	119	0.0943	1.58	10	1.67		2.738	112			6.10x
	GI	119	0.480	1.58	64	1.67		1.672	141			64.0
	GI	119	0.207	1.58	26	1.67		1.137	133			38.2
Barge	I	239	3.42	3.93	260	3.90		40.1	78?			25.3
	I	239	0.101	3.93	--	3.90		11.9	(132)			4.40x
	WI	239	1.94	3.93	323	3.90	16	48.3	165	0.477	79.7	26.1
	I	239	2.23	3.93	298	3.90		11.4	133			102
	GI	239	0.444	3.93	51	3.90		46.8	114			4.08x
	I	239	1.76	3.93	189	3.90		388.0	107			1.90x
	I	239	1.71	3.93	199	3.90		457.0	116			1.70x
	I	239	0.071	3.93	--	3.90		9.0	(132)			4.09x
	WI	532,481	1.07	14.6	226	10.7	44	11.34	186	0.358	54.5	213

? Questionable type designation or experimental error
x Subclass particles, presumably formed by collision of small active particle and large inactive particle
YS - yellowish sphere
WS - white sphere
YI - yellowish irregular
GI - greyish irregular
WI - white irregular

	Fused Particles	Irregular Particles (I)	Irregular Particles (II)
Average ma/cpm	83 x 10^{-17}	132 x 10^{-17}	--
Mean cpm/f	0.363 x 10^{-4} (± 38%)	0.363 x 10^{-4} (± 78%)	--
Mean ma/f	30.9 x 10^{-21} (± 38%)	118.6 x 10^{-21} (± 87%)	--
Mean ma/mg	803 x 10^{-11} (± 83%)	84.4 x 10^{-11} (± 108%)	2.91 x 10^{-11} (± 83%)
Mean Particle Mass, mg	--	3.36	26.4
Specific Activity, f/mg	26.0 x 10^{10}	0.471 x 10^{10}	0.0261 x 10^{10}

The fourth comparison between the spherical and irregular types of particles is by their specific activity. At H + 70, the ion current per milligram (mg) of the fused particles is about 15 times larger than that of the irregular particles. In this classification, the sample set of irregular particles is given an additional arbitrary subclassification by selection; the particles with a very low specific activity are separated out. The particles so selected for elimination are of the type found in the thin-section analyses where a small active particle is observed to be attached to a larger inactive coral grain. It is also possible that, had more particles been analyzed, the number distribution in specific activities could have filled in the intermediate values to give a broader single distribution.

The specific activity of the fused particles in terms of fissions per gram, based on Mo-99 yields, is about 55 times that of the irregular particles. Since the ion current per fission of the two types of particles becomes equal at about 6,000 hours after fission, the ion current from the fused particles is, on the average, 55 times larger than that of the irregular particles.

In a sense, the comparisons given should be taken with some reservation because of the small sampling. On the other hand, the large errors indicated by the standard deviations do not in themselves influence the validity of the conclusions from the data. These deviations rather indicate the breadth of the distributions in the radioactive content of the fallout particles or any other parameter of concern. Thus the single-particle data of this type are very useful; they provide detailed information on the likely nature of large-sample distributions.

The fractionation numbers for mass numbers 89 and 140, for some of the coral particles, are given in Table 2.8. The values given by Mackin and co-workers[35] are corrected to correspond to the yields from U-238 fission with 8-Mev neutrons. The values in the table show that, relative to mass 99, mass 89 was very much depleted in the fused particles and was enriched in some of the irregular particles. For mass 140, the enrichments in the irregular particles were as high as a factor of 4. In the irregular particles, the relative amounts of Sr-89 and Ba-140 were higher by factors of 21.0 and 21.9, respectively, than they were in the fused particles.

Correlations of fractionation numbers for fallout from relatively high-yield detonations on the surface of coral islands and on sea water are reported by Freiling.[38] In the report, Freiling mentions the identification of the induced activities of Na-24, S-35, Ca-45, Br-82, U-237, U-240, and Np-239, although no yields are given. The presence of the

Table 2.8

SUMMARY OF FRACTIONATION NUMBERS*
FOR MASS NUMBERS 89 AND 140 IN CORAL FALLOUT PARTICLES

Particle Description	GIC/f at H+70 (ma/f)x10^{21}	R^{89}_{90}	R^{140}_{99}	R^{140}_{99}/R^{89}_{99}
	A. Fused Particles			
WS	18.8	0.024	0.015?	0.625
S	18.8	0.012	0.030	2.50
YS	25.2	0.29	-	-
YS	26.9	0.026	0.028	1.08
S	29.0	0.0038?	0.018?	5.14
YI	32.8	0.046	0.14	3.04
YS	34.7	0.023	-	-
YI	35.0	0.041	0.14	3.41
WI	38.8	0.114	0.32	2.81
WI	40.7	0.23	-	-
WS	58.6	0.040	0.20	5.00
Geometric Mean	-	0.050(±180%)	0.10(±180%)	-
	B. Irregular Particles			
WI	54.9	1.81	0.82	0.453
WI	78.7	0.64	1.8	2.81
WI	88.6	0.36	-	-
GI	93.1	0.82	2.7	3.29
WI	120	1.0	4.0	4.00
WI	126	1.7	2.6	1.53
I	142	0.52	0.89	1.71
WI	203	2.3	3.6	1.56
GI	218	2.3	4.0	1.74
Geometric Mean	-	1.05(±98%)	2.19(±94%)	-

---

* R^{89}_{99}(U-238 fission) = 1.54 R^{89}_{99}(U-235 fission)

R^{140}_{99}(U-238 fission) = 1.17R^{140}_{99}(U-235 fission)

? Questionable values, not used to calculate means

last three nuclides suggests that much of the fission yield was due to the fission of U-238. The correlations indicate some relationship among the fractionation numbers, namely that, relative to the refractory elements, the fractionation numbers of the volatile elements increase or decrease more or less as a group. This could be due to the relative composition of the gross samples with respect to the two types of particles, as suggested by the data of Mackin for the coral fallout. It could also result from a time, concentration, and temperature dependence of the condensation process for each particle or particle group. The correlations therefore should depend on weapon yield and on type of environmental carrier material in forming the particles.

Freiling's treatment in correlating the data from all types of fallout together, irrespective of yield or carrier material, neglects these effects. The method of using the correlations is an artifact to spread out the data on a graph; however, such ratios are not required in the analysis of the data, and their use tends to depreciate the statistical reliability of the correlations because the variances are increased when ratios are taken. The data[38] are reproduced in Table 2.9 after being converted to fractionation numbers relative to mass number 99 and corrected to U-238 fission yields. The mass number 99 is used as the reference nuclide. For the samples in which the relative yields of the other refractory elements (Zr, Ce, U) are appreciably different from unity, indicating possible error in the data for mass number 99, one of the other refractory elements could be the chosen reference nuclide.

With corrections, the data indicate that:

1. Within experimental error, the mass numbers 95, 99, 144, 237, and 239 are present in their original ratios in all samples.

2. Only mass numbers with rare gas elements in the chain are fractionated in sea water fallout.

3. For the large yield detonation on the surface of deep sea water, the mass numbers with rare gas elements in the chain are not fractionated to a significant degree.

4. The fractionation numbers increase with (downwind) distance from shot point and therefore must decrease with the mean particle size.

5. The mass number 132, with the elements Sn, Sb, Te, and I in the decay chain, has fractionation numbers in the coral fallout that are nearly equal to those for mass number 90.

Table 2.9

SUMMARY OF FRACTIONATION NUMBERS RELATIVE TO MASS NUMBER 99
FOR CORAL AND SEA WATER FALLOUT CORRECTED FOR APPROPRIATE FISSION YIELDS

Relative Sample Location	Mass Number									
	89	90	95	99	132	137	140	144	237[a]	239[a]
A. Larger Yield (MT Range) Coral Surface Detonation										
Cloud Sample	5.1	4.0	2.1	(1.0)	2.5	3.3	4.2	2.0	1.2	1.2
	0.83	0.97	1.6	(1.0)	1.3	-	-	1.5	0.91	0.98
	0.38	0.44	1.0	(1.0)	0.69	0.22	0.88	0.96	0.78	0.87
	0.031	0.079	0.94	(1.0)	0.12	0.020	0.14	0.95	0.71	0.75
	0.13	0.24	0.82	(1.0)	0.45	0.046	-	0.88	0.73	0.75
	0.056	0.093	1.0	(1.0)	0.15	0.013	-	0.65	0.74	0.81
B. Large Yield (MT Range) Shallow Water Surface Detonation (Coral Bottom)										
Cloud Sample	2.1	2.1	1.4	(1.0)	1.5	1.7	2.2	1.2	1.0	1.0
	0.42	0.57	1.1	(1.0)	0.94	0.37	-	1.2	0.87	0.92
	0.65	0.74	1.5	(1.0)	1.3	0.20	-	1.6	1.0	1.1
	0.38	0.49	0.92	(1.0)	0.81	0.13	0.86	0.89	0.77	0.82
	0.082	-	0.51	(1.0)	0.27	-	-	0.60	0.56	0.63
	0.24	0.36	0.84	(1.0)	0.48	0.13	-	0.81	0.70	0.76
	0.12	0.18	0.84	(1.0)	0.34	0.062	0.42	0.70	0.72	0.71

Increasing Distance from Shot Point

a Values for 237 and 239 are not corrected for yields.

Table 2.9 (concluded)

	Relative Sample Location	Mass Number									
		89	90	95	99	132	137	140	144	237[a]	239[a]
	C. Medium Yield (KT Range) Surface Detonation on Deep Water										
	Cloud Sample	2.6	1.7	0.90	(1.0)	1.0	2.5	1.6	0.96	1.0	0.98
	↑	0.73	-	1.0	(1.0)	1.1	0.42	-	1.1	1.0	0.97
Increasing Distance from Shot Point		0.79	0.78	0.94	(1.0)	0.87	0.38	-	0.90	0.99	0.84
		0.46	0.47	1.3	(1.0)	0.98	-	0.70	1.1	1.1	0.98
		0.51	0.51	1.0	(1.0)	1.0	0.20	0.90	0.94	1.0	1.1
		0.30	0.57	1.1	(1.0)	0.99	-	-	1.0	1.1	0.98
	D. Large Yield (MT Range) Surface Detonation on Deep Water										
	Cloud Sample	1.1	-	1.2	(1.0)	0.77	-	1.0	1.0	0.98	1.0
	↑	1.2	0.99	1.1	(1.0)	1.0	-	-	1.3	0.94	0.97
Increasing Distance from Shot Point		0.96	0.93	1.1	(1.0)	0.95	0.41	-	0.92	0.86	0.96
		0.90	0.94	0.92	(1.0)	1.0	1.0	-	1.0	1.1	1.1
		0.53	0.80	1.5	(1.0)	1.0	1.2	-	1.1	0.64	0.71
		0.90	1.2	1.3	(1.0)	1.1	-	-	1.4	0.72	0.74
		1.6	1.2	0.95	(1.0)	1.1	-	-	0.94	0.72	0.74

Some idea of what occurred in the fallout formation process for mass numbers 89, 90, 137, and 140 can be deduced from the curves of Figure 2.12; these show the fraction of each chain that could have condensed at a given time after fission with the exception of the indicated elements. For the loss of rare gas members only, the minimum fractionation numbers for the four mass numbers are: 89, 0.16; 90, 0.36; 137, 0.24; and 140, 0.55. In this treatment, the fractionation numbers are relative to the independent yields of the chain and not to another mass chain yield; therefore values larger than 1 are not possible. However, the minima in the curves for the various mass chains occur at different times; therefore the maximum fractionation of all four mass chains would not be expected to occur for a given group of particles.

If the independent yields from Glendenin's postulate for U-235 fission are reasonably accurate estimates for the yields from a nuclear weapon, then, for condensation times up to 90 seconds, it appears from the data that only the alkaline earth members of the chains (Sr, Ba) and a fraction of the alkali metal elements (Rb, Cs) condensed in the coral particles falling nearest to shot point. For the condensation of like fractions of each element at any time up to 90 seconds after fission, the curves indicate that the fractionation number for mass number 90 should be larger than for mass number 89 and that its value for mass number 140 should be larger than for mass number 137.

The effect of increasing weapon yield on the condensation is to extend both the time and time-period over which the condensation occurs, since the rate of decrease of the fireball temperature decreases as the yield increases. On the average, the fallout from larger yield weapons therefore is less fractionated in mass numbers 89, 90, and 140 and even perhaps in mass number 137. The maximum amount of fractionation of these mass numbers results from condensations occurring between about 10 and 20 seconds after fission.

A plot of calculated fractionation numbers, $r_j(A, t)$, for mass numbers 90, 137, and 140, based on the independent yields of the chain members and the complete condensation of the alkali and alkaline earth nuclides, as a function of the $r_j(89, t)$ values for mass number 89, is shown in Figure 2.13. The shape of the curves suggests possible correlations among the fractionation numbers, especially if the condensation period is short. For times longer than about 30 seconds after fission, the curves for mass numbers 90 and 140 represent the case for noncondensation of only the rare gas chain members. If the condensation takes place over a relatively short time interval, the fractionation numbers are related according to

Figure 2.12
CALCULATED FRACTION OF MASS CHAINS 89, 90, 137, AND 140 CONDENSED AS A FUNCTION OF TIME AFTER FISSION WITH INDICATED NON-CONDENSING ELEMENTS.
(Based on Glendenen's Postulate of Independent Yields.)

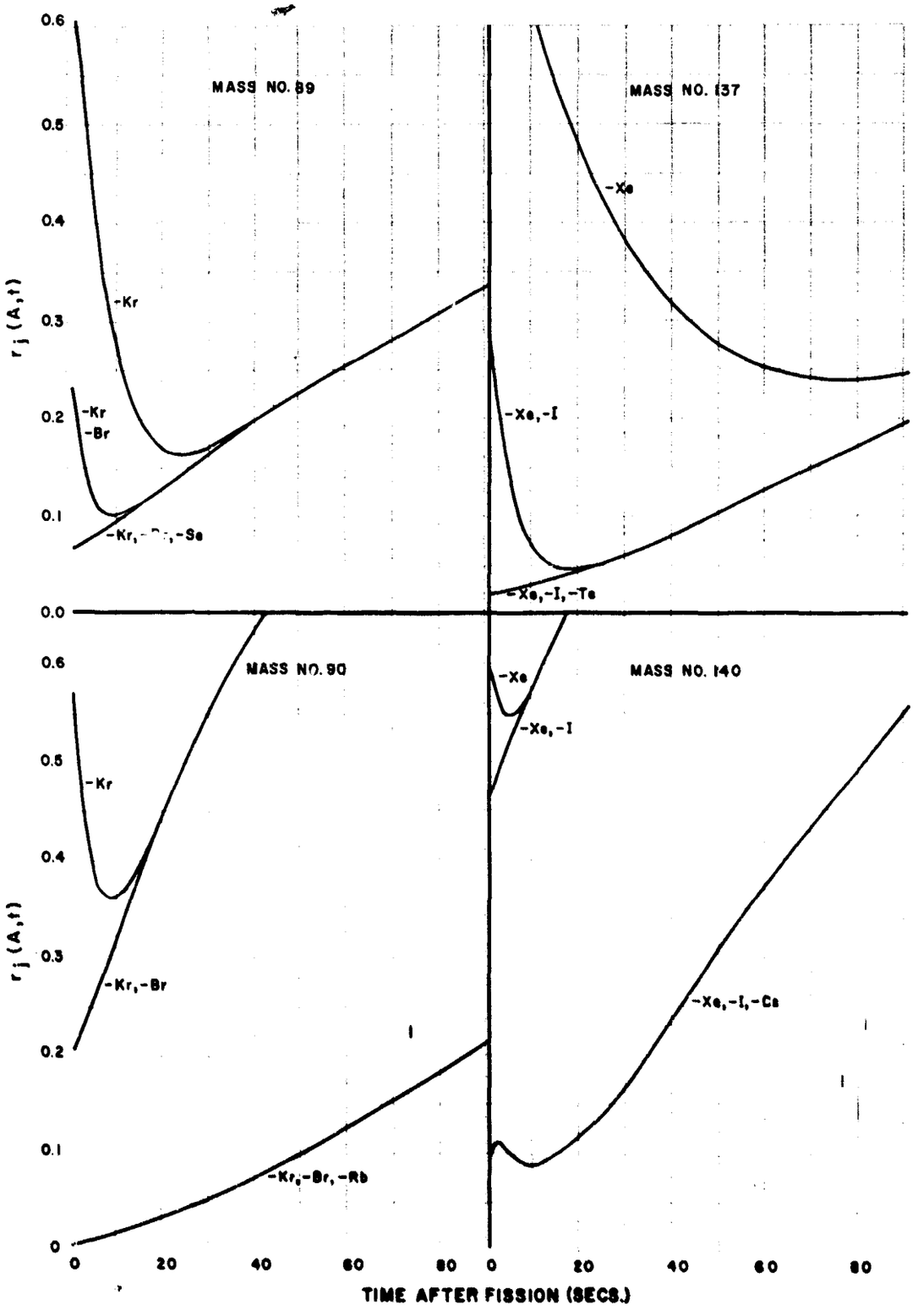

Figure 2.13
PLOT OF CALCULATED $r_j(A,t)$ VALUES FOR MASS NUMBERS 90, 137, AND 140 AGAINST THOSE OF MASS NUMBER 89 FOR THE ASSUMPTION THAT ONLY THE ALKALI METAL ELEMENTS AND ALKALINE EARTH ELEMENTS IN THE CHAIN CONDENSE

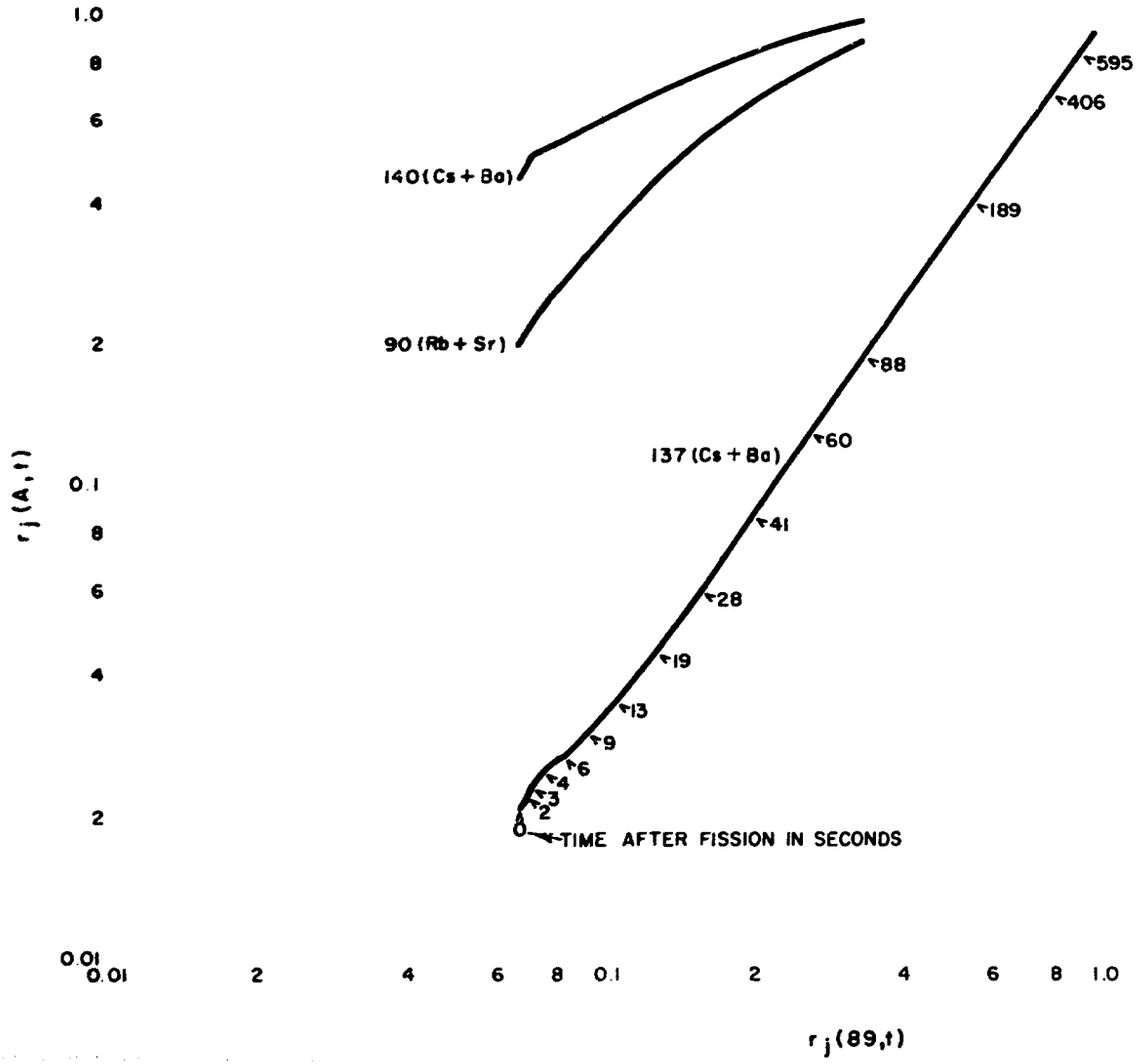

$$r_j(A, t) = r_o(A) \left[r_j(89, t) \right]^n \qquad (2.1)$$

where $r_o(A)$ and n are constants; the constant n is the slope of the curve for a short period of time.

The empirical correlation constants for Equation 2.1 are given in Table 2.10, along with the mean values of the condensation times taken from a plot of $r_o(A)$ and n as derived from the tangents to the $r_j(A, t)$ curves in Figure 2.13, with time after fission; $r_o^*(A)$ is the coefficient for the observed data. The mean times of condensation range from about 25 to 50 seconds after fission and agree reasonably well considering the scatter in the data. More precise data would permit estimating the fractionational condensation of the alkali metal elements and even perhaps of iodine in the case of mass number 137. However, the results of the treatment give reasonable values of the times at which the condensation occurred.

The main feature of this type of data correlation is the notion that the fractionation numbers of the volatile elements vary in some uniform manner, so that if one element is fractionated all other elements are also fractionated to a degree specified by the empirical correlations. Unfortunately, the method requires the fractionation number of at least one mass number in addition to the analysis of a reference nuclide before it can be utilized to make estimates of the fractionation number of other radionuclides. In addition, a sufficient number of mass numbers correlations are not reported from which to estimate the gross decay and the potential dose from fallout.

The average fractionation numbers for some radionuclides in the fallout from tower and balloon-supported detonations are given in Table 2.11, as derived from data reported by Larson and Neel.[13] The values are given relative to the refractory Zr-95 nuclide and to the mass chain yields for thermal neutron fission of U-235. The data presumably apply to the smaller fallout particles with diameters less than about 100 microns. The values of the fractionation numbers for the fallout from the tower-mounted explosions suggest that the Zr-95 condensed more completely on the collected particles than the nuclides Sr-89, Sr-90, and Ru-103(106).

In the smaller particles from the balloon-mounted explosions, the relative fractionation numbers of all the reported nuclides are greater than unity, indicating enrichment of the nuclides Sr-89, Sr-90, Y-91, Ru-103(106), Ba-140, and Ce-141 with respect to the Zr-95. Thus, unless

Table 2.10

COMPARISON OF EMPIRICAL FRACTIONATION-CORRELATION PARAMETERS WITH THOSE ESTIMATED FOR CONDENSATION OF ALKALI AND ALKALINE EARTH ELEMENTS OF MASS CHAINS 90, 132, 137, AND 140, AT SPECIFIED TIMES AFTER FISSION

Mass Number	Data Source	$r_o^*(A)$	n	t(sec)	$r_o(A)$
90	Shot A	1.12	0.77	34[a]	2.25
	Shot B	1.09	0.82	31[a]	2.43
	Shot C	0.91	0.66	47[a]	1.85
132	Shot A	1.51	0.80	-	-
	Shot B	1.70	0.75	-	-
137	Shot A	0.90	1.46	36[a], 35[b]	0.90, 0.88
	Shot B	0.71	1.19	25[b]	0.71
	Shot C	0.57	1.55	39[a]	1.05
140	Shot A	1.60	0.62	38[b]	1.60
	Shot B	1.44	0.58	52[b]	1.44
	Shot C	1.08	0.42	35[a]	1.65

a From n vs t; (t is the estimated time of condensation)

b From $r_o(A)$ vs t

Table 2.11

AVERAGE FRACTIONATION NUMBERS OF RADIONUCLIDES IN FALLOUT FROM TOWER AND BALLOON-SUPPORTED DETONATIONS AT THE NEVADA TEST SITE

Nuclide	R(95)[a]	
	Tower	Balloon
Sr-89	0.32	1.5
Sr-90	0.65	-
Y-91	1.4	2.8
Zr-95	1.0	1.0
Ru-103(106)	0.45	3.2
Ba-140	1.4	3.5
Ce-141(144)	1.4	2.3

a Relative to the yields for thermal neutron fission of U-235.

unexpected errors occurred in the analyses for the Zr-95 nuclide, a high degree of separation between the very refractory and the volatile fission-product elements occurs in the fallout from air bursts as well as in the fallout from near-surface bursts. The relative enrichment of the volatile nuclides (or daughters of volatile nuclides) in the smaller particles from the balloon-mounted explosions is similar to the behavior for the small particles in the fallout from the near-surface explosions.

2.5 The Condensation Process

2.5.1 General Description

The essential features of the fallout formation process deduced from the final structures, compositions and general properties of fallout particles as described in the previous sections are that:

1. Some portion of the radioactive elements condenses into liquid particles.

2. Some portion condenses onto the surface of solid particles.

3. If a time limit is placed on the process, some fraction of some of the radioactive elements will be still in the vapor phase.

Even in the case where the bulk carrier is sea water, the first two statements are valid for the fallout from a moderately high-yield detonation near the sea surface since the temperature of the drops, at the altitude of the cloud, will at some time fall below freezing.

The condensation process in fallout formation can be divided into two general time periods. The first period of the process is characterized by the presence of gas and liquid phases and the second period by the existence of gas and solid (or cool glass) phases. The first period of condensation ends when the bulk carrier particles become very viscous and/or solidify; the end of the first period of condensation is more precisely defined perhaps by the temperature of the glassy particles at which diffusion into the particles becomes very low. There is probably no real precise instant at which this occurs in the fireball since temperature gradients must certainly exist; it is highly likely that the different sizes of particles cool (and solidify) at different rates and times.

One most important aspect of the condensation of the radioactive fission products into the liquid phase is that the fission-product elements and compounds are dissolved to form a very dilute solution. Because of this dilution, the solution process can be treated with neglect of (a) surface saturation effects and (b) interactions among the various radioactive elements in the formation of the solution.

In a glassy matrix, i.e. after "solidification," the dissolved or compounded fission products should not be able to escape. With concentrations of the order of 10^{-10} moles of fission products per mole of glass, the vapor pressure would be extremely low, and the diffusion of the elements through the solid glass would be very slow.

The fraction of each fission product that is condensed into the liquid carrier particles when they solidify will be determined by (a) the melting point of the carrier and (b) the time after fission at which the solidification occurs. If the melting point of the carrier is high, the fractions that are condensed will be smaller than those in carrier materials having low melting points. For some of the larger particles, the fractions that are condensed will be determined by the time at which solidification of the particle occurs. In the case where the carrier can exist in the liquid state over a relatively large temperature range and the yield is reasonably large so that fireball does not cool too rapidly, the larger particles can not only enter but can leave the fireball volume before the interior gases cool to the temperature at which the particles solidify.

The fraction of each fission product that is not condensed into the liquid phase of the carrier can still condense on or react with the surface of the solid particles. The solid particles available could consist of (a) the smaller of the melted particles (since these do not fall out of the cloud volume as soon or as rapidly as the larger particles) or (b) of unmelted particles that enter the gas volume at later times.

The best illustration of the latter type of particle is the irregular particles found in the coral fallout. Because of the high melting point of calcium oxide, the number of the more active (fused, spherical) particles found was usually, but not always, smaller than the number of irregular unmelted particles. Even though the fused particles had higher specific activities, they carried a fraction of the total radioactivity produced that was much smaller than the fraction carried by the irregular unmelted particles.

The reverse was true for the particles of the lower-melting silicate glasses. There is no doubt that both unfused and sintered grains of soil

and the smaller fused spheres carried radioactivity on their surfaces; various amounts of activity were leached from the samples of these particles in water and dilute acids. However, in the presence of the larger fused spheres in heavy fallout regions, the irregular soil grains contributed only a rather small fraction of the total radioactive content of the fallout deposit.

In the second period of condensation, i.e. after the particles solidify, the fission-product elements may condense by (a) sublimation on the surface of solid particles or (b) they may react directly with the carrier substance. In the case of a more or less open or porous crystal structure, the fission products could diffuse well into the body of the particle. This process was evidenced by the layer of activity in the irregular coral particles.

The previously mentioned vapor-condensation computations using simple kinetic theory, or the more complicated method used by Stewart,[6] both indicate that condensation-vaporization equilibrium can be established within a fraction of a second at temperatures around 2000°K. The finding of the small spheres in fallout collections confirms the nature of this early direct vapor-condensation. When equilibrium is established, the gaseous species of each fission product element can either (a) react with the vapor or liquid products of the bulk carrier or (b) dissolve into the liquid phase according to Henry's law of dilute solutions. These solutions of fission product elements or compounds in the liquid phase should be (a) sufficiently dilute to result in no change in the free energy of the liquid carrier and (b) so dilute that the free energy of solution of each element is independent of the concentration of all other fission-product elements.

The origins of the melted particles in the fireball may be several in number. The small vapor-condensed particles originating from vaporized soil have been mentioned. Others are the particles that were originally lying on the ground out to some distance from shot point, some of which probably are warmed and perhaps melted by the heat absorbed from the radiant energy emitted at detonation. These particles are then drawn into the fireball as it rises.

In low air bursts, where a very small crater is formed, the latter mechanism probably is the dominant process by which particles enter the fireball. In this case the size distribution of the fallout particles that are produced should be the same as the original size distribution of the surface soil. In the detonation, the blast wave would powder the surface layer of soil to some depth and the resulting dust particles, like the surface-melted particles, would retain their size in the

formation process. However, these particles would not be melted until after they entered the fireball.

For surface detonations, two other major mechanisms may occur that cause particles to enter the fireball. One is the "jetting" of the soil where the blast or shock wave hits the soil surface; this should occur at very early times after detonation. The soil grains in the jets may be partially heated or even melted by absorption of energy from the blast wave and then vaporized as they penetrate into the hot fireball gases at high velocity. Following this ejection of the surface layers of soil material, new exposed but thin layers of soil may be melted. It seems reasonable that such a liquid layer of soil would intervene between the vapor in the fireball and the layer of shock-powdered earth as long as the fireball remained in contact with the earth's surface. If enough "fluxing" material (such as the carbonates) is present, a rather large amount of fluid material could be formed. The other major mechanism takes place as the fireball lifts; the liquid is broken up into drops that enter the fireball, followed by the powdered soil. The mechanical break-up of the fluid mass should produce about the same size distribution of particles from all liquids that have about the same surface tension.

2.5.2 Gas-Liquid Phase Condensation

Because of the extreme dilution of the fission product elements in the fallout particles, it is possible to consider the gas-liquid phase condensation and the solubility of each fission product element in the carrier as an independent two-component system. Moreover, there should be no appreciable surface loading (due to large excess surface concentrations during the condensation process) if the temperature range over which the liquid carrier exists exceeds 200 or 300°C. Concentration gradients in particles may occur, however; particles that are not heated very much above the softening temperature and are not very fluid, or larger particles that may not have been melted in their center by the time the surface temperature falls below the melting point, would each contain concentration gradients when solidified.

Two general types of gas-liquid phase condensation processes may be considered. One is Henry's law of dilute solution; the other is compound formation with carrier material. Henry's law of dilute solution is given by

$$p_j = k_j N_j \qquad (2.2)$$

in which N_j is the mole fraction of element j in the liquid phase, k_j is the Henry's law constant, and p_j is the partial pressure of the gaseous species of element j. For a mixture of gases

$$p_j = N_j^o P \tag{2.3}$$

in which N_j^o is the mole fraction of the gaseous species of element j in the vapor and P is the total pressure. Combining Equations 2.2 and 2.3 gives

$$N_j^o/N_j = k_j/P \tag{2.4}$$

If the liquid soil particles are assumed to be more or less uniformly distributed throughout the fireball volume, and the temperature is also assumed to be somewhat uniform, then all the liquid particles may be considered as a single liquid phase in contact with the gas at a given temperature and time. Although a given pair of values of P and T at a given time would be valid only for some small increment of the fireball volume, it is obvious that these cannot be given; a uniform or average value for the whole volume is assumed in the treatment.

Without specifying the number or size of particles, the mole fraction of element j in the liquid phase is given by

$$N_j = n_j/n(\ell) \tag{2.5}$$

where n is the number of moles of element j dissolved in $n(\ell)$ moles of liquid carrier where $n_j \ll n(\ell)$. The mole fraction of element j in the vapor phase is given by

$$N_j^o = n_j^o/n \tag{2.6}$$

where n_j^o is the number of moles of element j mixed with n moles of vapor and $n_j^o \ll n$.

If the perfect-gas law is assumed for all the gaseous species comprising the n moles of gas, n_j^o is given by

$$n_j^o = \frac{n_j k_j}{\left[n(\ell)/V\right]RT} \qquad (2.7)$$

The ratio, n_j^o/n_j, in Equation 2.7 depends on the values of k_j, T, and $n(\ell)$ per unit volume in the fireball at the time.

Because the mole fractions are small, the value of n_j^o/n_j is independent of the total amount of the element present. Therefore the same fraction of an element should be condensed at a given time and temperature for a 100 percent fission weapon as for a "clean" thermonuclear weapon of the same total yield. The value of $n(\ell)/V$ depends on the total yield and time after detonation, since the amount of carrier material liquified depends on (a) how the total energy is utilized in the process and (b) the rate of the in-flow and spatial distribution of the carrier material passing through the fireball volume.

Compound formation of an element with the carrier in the gas phase, followed by condensation of the heavier gas molecule into a liquid solution with the melted carrier material, can also be described by use of Henry's law for the dilute solution. However when the compound is formed with the (bulk) liquid carrier, then the free energy of formation of the compound and its heat of vaporization must be considered. The over-all reaction for this condensation process is

$$A(g) + xO_2(g) + B(\ell) \rightarrow AO_{2x}B(\ell), \text{ dilute solution in } B(\ell)$$

in which x is the number of oxygen molecules that combine with each atom of element A. For this reaction,

$$n_A/n_{AOB} = \frac{k_{AO}\, e^{\Delta F^o/RT}}{\left[n(\ell)/V\right]RTp^x(O_2)} \qquad (2.8)$$

where n_A is the number of atoms in the gas phase, n_{AOB} is the number of atoms of AO_{2x} in dilute solution, k_{AO} is the thermodynamic activity coefficient for AO_{2x}, ΔF^o is the standard free energy for the condensation process, and $p(O_2)$ is the oxygen partial pressure. Equation 2.8 is the same as Equation 2.7 for a simple condensation reaction except for the dependence on the oxygen pressure.

Application of material balance constraints for the number of atoms of a fission product element in a mass chain gives, for the fraction of the mass chain condensed or the absolute fractionation number of each number of the chain,

$$r_j(A, t) = \frac{1}{Y_A} \Sigma_j n_{jA}(t) \qquad (2.9)$$

where Y_A is the mass chain yield and $n_{jA}(t)$ is the number of atoms of element j of mass A that is condensed into the liquid phase at the time t. With Henry's Law constant, the fractionation number of each member of the mass chain A becomes

$$r_j(A, t) = \Sigma_j \frac{y_j(A, t)}{1 + k_j^o} \qquad (2.10)$$

where k_j^o represents $k_j / \left[(n(\ell)/V)RT \right]$ and $y_j(A, t)$ is the fractional mass chain yield of element j at the time t after fission. The fraction of each neutron-induced activity for both the weapon construction and environmental materials that is condensed into the liquid phase of the particles is given by

$$r_j(t) = \frac{1}{1 + k_j^o} \qquad (2.11)$$

For an induced parent radionuclide, $r_j(t)$ depends only on k_j^o since the number of atoms condensed changes at the same rate as those not condensed.

2.5.3 Gas-Solid Phase Condensation

In the second period of condensation, the fraction of each element not condensed from the gas phase (when the fireball temperature has fallen below the melting point of the carrier material) can begin plating out on the surface of solid particles. The available particles for this period of condensation can be the smaller solidified particles that have not settled out of the radioactive gas volume plus the unmelted soil grains that entered the fireball late and were not heated to their

melting temperature.

Although it is possible that a variety of gas-solid state reactions may occur for the different elements, depending on the physical and chemical properties of the carrier particles, only one simple and idealized process is considered here. This is that the fraction of each element that is condensed, up to some stated time after fission, is related to that element's total sublimation pressure. Further, it is assumed that the carrier surface acts as if it were the pure solid compound of the condensing species. Under these conditions, the computational values of the amounts condensed reflects the relative volatility of the (assumed) constituent gaseous molecules at all temperatures at which this kind of condensation can occur.

The fractionation number of the end-chain member of each mass chain, or the fraction of the chain that is condensed up to a given time in the second period of condensation, $r'_j(A, t')$, is defined by

$$r'_j(A, t') = \Sigma_j \frac{y_j(A, t)k^o_j}{1 + k^o_j} - \frac{V'}{RT'} \Sigma_j p^s_j(A, t') \qquad (2.12)$$

in which

$$p^s_j(A, t') = \frac{p^s_{jA}}{0.241 Y_A BW} \qquad (2.13)$$

where Y_A is the (fractional) chain yield in atoms per fission, B is the ratio of fission to total yield, W is the total yield in kilotons, the total chain yield is $0.241 Y_A BW$ moles, p^s_{jA} is sublimation partial pressure of element j of mass number A, V' is the cloud volume at t', and T' is the temperature at t'.

In Equation 2.12, the k^o_j values are, as in Equation 2.10, evaluated at the temperature of the end of the first period of condensation; this is different from the temperature T' in the second term. Thus the fractions of each element not condensed during the first period of condensation (given by the first term of Equation 2.12) must be decay-corrected to the time of interest to determine $p^s_j(A, t')$.

The fractionation number of the neutron-induced radionuclides for the second period of condensation is given by

$$r_j'(t') = \frac{k_j^o}{1 + k_j^o} - \frac{p_{jA}^s V'}{n_j(t')RT'} \qquad (2.14)$$

in which $n_j(t')$ is the total number of moles of the element designated by j involved in the formation of fallout. For nuclides formed by (n, γ), (n, 2n), and (2n, γ) neutron reactions with weapon construction materials, $n_j(t')$ is the number of moles of the element present when the weapon detonates. For the radionuclides formed similarly from soil environmental materials, $n_j(t')$ is the number of moles of the element initially vaporized in the detonation. The value of $n_j(t')$ for radionuclides formed by capture processes other than the three above neutron reactions requires information on the relative yields of the capture products.

The term $p_{jA}^s V'/RT'$ is the maximum number of moles of element j that could be present in the volume V' for a saturated vapor at the temperature T'. In the case that this number is larger than the number of moles of available uncondensed atoms, none of them would condense. For such conditions, $r_j'(t)$ would be zero even though its computed value in Equation 2.14 could be a large negative number.

2.5.4 Particle-Size and Fractionation

In the discussion of the condensation processes, some attention must be given to the effect of particle size on the amount of the element condensed. The vapor pressure over the liquid drops can depend on the size of the drop, especially at the higher temperatures. However, the influence of surface tension of oxides and glasses on the partial pressure at temperatures of interest is negligible for particles with diameters greater than a few tenths of a micron. Hence liquid surface tension cannot cause differences in fractional condensation for particles of different sizes.

Thus the variations with distance, or with particle size, that are found in the fractionation numbers in the data (see Sections 2.2 and 2.3) must arise from other causes. The major cause appears to be the difference in the period of time that the different-sized particles stay in the gas volume. The toroidal circulation which can eject the larger

particles at the earlier times after detonation, as a cause of fractionation variations with particle-size, is discussed in Chapter 3.

CHAPTER 2 REFERENCES

1. The Effects of Nuclear Weapons, U.S. Government Printing Office, Washington 25, D.C. (1957); revised 1962

2. Adams, C. E., I. G. Popoff, and N. R. Wallace, The Nature of Individual Radioactive Particles, I: Surface and Underground ABD Particles from Operation Jangle, USNRDL-374, 1952

3. Maxwell, Ray D., Project 2.5a-3 Report, Operation Jangle, 1952

4. Schorr, M. G., and E. S. Gilfillan, Project 2.0 Report, Operation Jangle, 1952

5. Alexander, L. T., J. M. Blume, and M. E. Jefferson, Project 2.8 Report, Operation Jangle, 1952

6. Stewart, K., Trans. Faraday Soc., Vol. 52, 161 (1956)

7. Pettijohn, F. J., Sedimentary Rocks, Harper Brothers, New York, N.Y., 1949

8. Adams, C. E., The Nature of Individual Radioactive Particles, II: Fallout Particles from M-Shot, Operation Ivy, USNRDL-408, 1953

9. Adams, C. E., N. H. Farlow, and W. R. Schell, Geochimica et Cosmochimica Acta, Vol. 18, 18 (1960)

10. Adams, C. E., and J. P. Wittman, The Nature of Individual Radioactive Particles from an ABD of Operation Upshot-Knothole, USNRDL-440, 1954

11. Adams, C. E., and J. D. O'Connor, The Nature of Individual Radioactive Particles, VI: Fallout Particles from a Tower Shot, Operation Redwing, USNRDL-TR-208, 1958

12. Farlow, N. H., Analyt. Chem., Vol. 29, 883 (1957)

13. Nishita, Hideo. and K. H. Larson, Summary of Certain Trends in Soil-Plant Relationship Studies of the Biological Availability of Fallout Debris, UCLA-401 (1957)

14. Larson, K. H., and J. W. Neel et al, Summary Statement of Findings to the Distribution, Characteristics, and Biological Availability of Fallout Debris Originating from Testing Programs at the Nevada Test Site, UCLA-438, 1960

15. Fuller, R. K., unpublished data, USNRDL, 1960

16. Romney, E. M., R. G. Lindberg, H. A. Hawthorne, B. G. Bystrom, and K. H. Larson, Health Physics (to be published)

17. Nishita, Hideo, E. M. Romney, and K. H. Larson, Agricultural and Food Chemistry, Vol. 9, 2, 101 (1961)

18. Lindberg, R. G., et al, The Factors Influencing the Biological Fate and Persistence of Radioactive Fallout, Operation Teapot, WT-1177, 1959

19. Rainey, C. T., et al, Distribution and Characteristics of Fallout at Distances Greater than Ten Miles from Ground Zero, March and April, 1953, Operation Upshot/Knothole, WT-811, 1954

20. Bolles, R. C., and N. E. Ballou, Calculated Abundances of U-235 Fission Products, USNRDL-456, 1956

21. Katcoff, Seymour, Nucleonics, Vol. 16, 4, 78 (1958)

22. Katcoff, Seymour, Nucleonics, Vol. 18, 201 (1960)

23. Weaver, L. E., P. O. Strom, and P. A. Killeen, Estimated Total Chain and Independent Fission Yields for Several Neutron-Induced Fission Processes, USNRDL-TR-633, 1963

24. Glendenin, L. E., Technical Report No. 35, Massachusetts Institute of Technology, Cambridge, Mass., 1949

25. Steinberg, E. P., and L. E. Glendenin, International Conference on The Peaceful Uses of Atomic Energy, Vol. 7, 3 (1956)

26. Pappas, A. C., International Conference on The Peaceful Uses of Atomic Energy, Vol. 15, 583 (1958)

27. Wahl, A. C., J. Inorg. Nucl. Chem., Vol. 6, 263 (1958)

28. Glendenin, L. E., C. D. Coryell, and R. R. Edwards, Radiochemical Studies: The Fission Products, NNES, Plutonium Project Record, Div. IV, Vol. 9, 489, McGraw Hill, New York, N.Y., 1951

29. Herrington, A. C., Massachusetts Institute of Technology, Laboratory for Nuclear Science, Annual Progress Report, June 1957 - June 1958, p. 37

30. Coryell, C. D., M. Kaplan, and R. D. Fink, Can. J. Chem., Vol. 39, 646 (1961)

31. Leachman, R. B., Phys. Rev., Vol. 101, 1005 (1956)

32. Miller, C. F., A Theory of Formation of Fallout, USNRDL-TR-425, 1960

33. Kimura, Kenjiro, Geneva Conference on The Peaceful Uses of Atomic Energy, Vol. 7, 196 (1956)

34. Miller, C. F., Fallout and Radiological Countermeasures (Vols. I and II), Stanford Research Institute, Project IMU-4021, January 1963

35. Mackin, J., P. Zigman, D. Love, D. McDonald, and D. Sam, J. Inorg. Nucl. Chem., Vol. 15, 20 (1960)

36. Jones, J. W., and R. T. Overman, AECD-2367, 1948

37. Miller, C. F., and P. Loeb, Ionization Rate and Photon Pulse Decay of Fission Products from the Slow Neutron Fission of U-235, USNRDL-TR-247, 1958

38. Freiling, E. C., Fractionation Correlations, USNRDL-TR-385, 1959